SOVIET SCIENTIFIC REVIEWS/SECTION C

Mathematical Physics Reviews

Edited by S.P. Novikov, Guest Edited by Ya. G. Sinai
L.D. Landau Institute of Theoretical Physics, USSR Academy of Sciences, Moscow

VOLUME 8, PART 4

Universal Scenarios of Transitions to Chaos via Homoclinic Bifurcations

D.V. Lyubimov
A.S. Pikovsky
M.A. Zaks

Soviet Scientific Reviews are published by harwood academic publishers

SOVIET SCIENTIFIC REVIEWS

A series of journals publishing the most significant developments in the important research areas of Soviet science. In making these publications available, the publisher hopes to contribute to the further development of international cooperation between scholars and to a greater understanding among scientists.

MATHEMATICAL PHYSICS REVIEWS

edited by S.P. Novikov, L.D. Landau Institute of Theoretical Physics, USSR Academy of Sciences, Moscow

Section C of Soviet Scientific Reviews

GENERAL INFORMATION

Aims and Scope. MATHEMATICAL PHYSICS REVIEWS publishes review articles covering significant developments in Soviet mathematical physics research, written by eminent experts in the field.
It is intended to make accounts of recent scientific advances in the USSR readily and rapidly available to Western scientists who do not read Russian.

Publication Schedule. Most issues of MATHEMATICAL PHYSICS REVIEWS will be self-contained and will cover a single topic. Issues are available individually as well as by subscription. Each volume is comprised of approximately 400 pages with an irregular number of parts (depending upon size) scheduled.

Subscription rates

Each volume is composed of approximately 400 pages with an irregular number of parts (depending upon size) scheduled. Issues are available individually as well as by subscription.
Subscription rates per volume: corporate, $224.00; university library, $140.00. Rates include air mail postage and handling charges. Individual subscription rates are available only to individuals who subscribe directly from the publisher and who pay through personal checks or credit card.
Prices apply in North America only. All other countries will be invoiced at our current conversion rate. The subscription rates include a distribution charge of $20.00 for postage and handling. Send your order to your usual supplier or direct to Harwood Academic Publishers GmbH, c/o STBS Ltd, 1 Bedford Street, London WC2E 9PP, England. Claims for nonreceipt of issues should be made within three months of publication of the issue or they will not be honored without charge. Subscriptions are available for microform editions. Please write for details.

Distributed by STBS Ltd, 1 Bedford Street, London WC2E 9PP, England and Post Office Box 786, Cooper Station, New York, New York 10276, USA. Printed in the United Kingdom by Bell and Bain Ltd, Glasgow.

APRIL 1989

UNIVERSAL SCENARIOS OF TRANSITIONS TO CHAOS VIA HOMOCLINIC BIFURCATIONS

CONTENTS

Sov. Sci. Rev. C. Math. Phys. Vol. 8, 1989, pp. 221–292

Printed in the United Kingdom

UNIVERSAL SCENARIOS OF TRANSITION TO CHAOS VIA HOMOCLINIC BIFURCATIONS

D.V. LYUBIMOV[1], A.S. PIKOVSKY[2] and M.A. ZAKS[3]

[1]*Perm University, Perm, USSR*
[2]*Inst. Applied Physics, USSR Academy of Sciences, Gor'ky, USSR*
[3]*Inst. Mechanics of Continuous Media, USSR Academy of Sciences, Perm, USSR*

Abstract

The behavior of bifurcation sequences connected with the occurrence of trajectories that are doubly-asymptotic to saddle states of equilibrium in the phase space of dynamic systems are investigated. The structure of parameter space is analyzed using renormalization group methods and also using examples of numerical and qualitative investigations of discrete and continuous models. The bifurcation diagram possesses the properties of self-similarity while the boundary of chaos is fractal. Two types of similarity on this boundary are distinguished and investigated, similar to the well-known structures for period doublings and quasi-periodicity. It is found that in a number of situations the corresponding RG transformation has a singular fixed point, which leads to super-exponential convergence of the bifurcation sequence.

1. INTRODUCTION

The laws governing transition from regular to chaotic (stochastic) motions are of great interest in various problems of hydrodynamics, non-linear optics, and chemical kinetics, etc. The scenarios of such transition that have been most fully studied theoretically and observed experimentally include the following. First, there is the well known sequence of period-doublings of stable oscillations [1, 2]. Second, there is the transition to chaos via intermittency, i.e., the alternation of regular and chaotic behavior of a system [3, 4], due to disappearance of the stable periodic state [5]. Another popular scenario is linked with destruction of the invariant tori [6], and the transition here occurs via a quasi-periodic motion [7, 8].

More exotic situations have been discussed in the literature, such as period-tripling [9], III-type intermittency [3], and the tricritical point of period-doubling [10], etc. A feature in most of these problems is the analogy between the transition to chaos and phase transition, for which there are both physical and mathematical reasons.

Physically, the analog of the order parameter in the transition to chaos problem is the Lyapunov characteristic exponent λ, which defines the rate of divergence of adjacent phase trajectories [11]. Noting that λ has the dimensionality of inverse time, λ^{-1} is proportional to the time scale of stochastization. At the transition point $\lambda = 0$, and the characteristic time of stochastization tends to infinity, while in the neighborhood of this point it is much greater than the other time scales (period, etc.). Thus the transition to chaos occurs in a universal manner which is independent of the details of the concrete system, just as, at a point of phase transition, where the characteristic spatial scale of the fluctuations is much greater than the inter-atomic distance, the dependence on the details of atomic interaction disappears.

The mathematical reason for the analogy is the scale invariance and the renormalization group (RG) method based on it. Feigenbaum [1, 2] was the first to apply RG methods to the problem of transition to chaos, by describing the universal properties of the sequence of bifurcations of period-doubling. This approach was then used for studying other transition scenarios, see e.g., [7, 8], and critical phenomena in dynamic systems [12, 13]. Actually, the results of renormalization analysis are characteristics of the objects (points, manifolds, etc.), which are

invariant under a transformation in the parameter space of the dynamic system; in the neighborhood of these objects the sequences of bifurcations have self-similarity properties that are universal, i.e., independent of the system details.

We shall be concerned in the present paper with transitions in dissipative dynamic systems with saddle equilibrium states. We confine ourselves to the case when only one eigenvalue λ_1 of the linearization matrix close to the saddle point lies in the right half-plane, while the rest are in the left half-plane. The unstable manifold W^u is then one-dimensional and consists of the point itself and a pair of trajectories "departing" from it, which we call below separatrices Γ_1 and Γ_2. The stable manifold W^s has co-dimension 1. This situation is typical for many physical problems, when, as a result of variation of the parameters, the stationary mode loses stability with respect to monotonous increasing perturbations: an example is the crisis of mechanical equilibrium in the Rayleigh–Benard problem of the convective instability of a liquid layer heated from below. We shall assume that, remote from the saddle, the two separatrices come close to W^s and return along it to the saddle zone (Fig. 1). Such behavior is well known from the Lorenz model [14]; but we shall not impose the condition, typical for this

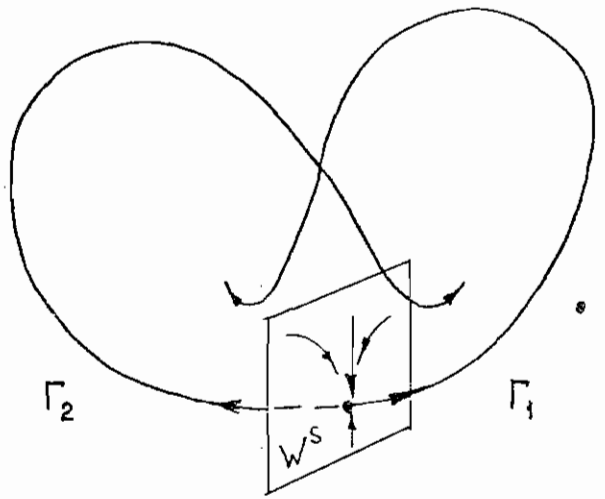

Figure 1 Return of separatrices to neighborhood of saddle point.

model, that the separatrices be symmetric to one another.

When the parameters move slightly, each separatrix can be captured by a stable manifold, forming a trajectory (homoclinic loop) which is doubly asymptotic to the saddle. To this event in the parameter space there corresponds a surface of co-dimension 1. The rigorous theory of the bifurcations that accompany the appearance of different types of single loops, and the required mathematical apparatus, was developed by Shilnikov [15–17]. It turns out that the picture essentially depends on whether the eigenvalue λ_2, corresponding to the most slowly damped perturbations (i.e., the most right in the left half-plane), is real or complex. In the latter case the equilibrium is of the saddle-focus type. The loop formation (under certain auxiliary conditions) then indicates the existence of a hyperbolic set [16], and at close values of the parameters, sequences of period-doubling bifurcations are observed, along with the merging of stable and unstable periodic solutions, and other effects, see [18–21] for details.

We shall confine ourselves, however, to the case when λ_2 is real, and the real mode damps more slowly than the others. Shilnikov [17] showed that here, when the single homoclinic loop breaks up, only single closed phase trajectory is formed, the stability of which is determined by the sign of $\lambda_1 + \lambda_2$. In the situation when the two separatrices return to the saddle, however, more complicated structures can arise, as exemplified by the Lorenz system. Here, $\lambda_1 + \lambda_2 > 0$, and destruction of the pair of homoclinic loops leads to the formation of a complicated non-attracting set, which consists of a countable number of periodic solutions and a continuum of trajectories, doubly asymptotic to them [22, 23]. Though the dynamics in this set are chaotic, such behavior can only be observed as a transient motion (metastable chaos [24]). With a change of the parameters the chaotic set may become stable, converting into a Lorenz attractor. This scenario has been studied several times; for the most complete analysis, see Afraimovich, Bykov, and Shilnikov [25]; references to studies of the Lorenz system can be found in Sparrow [26].

In the case of a negative saddle quantity $\lambda_1 + \lambda_2$, stable limit cycles follow the destruction of homoclinic loops. The fact that the two separatrices return in the neighborhood of the saddle, i.e., trajectories do not leave the saddle without returning, means that we can trace the bifurcations of these cycles and study other motions that are possible here, which is in fact the main object of our study.

A rigorous mathematical consideration of dynamic systems fairly close to a system with a pair of homoclinic trajectories was given by Turaev and Shilnikov [27], where the attracting sets corresponding to regular motions were characterized. In order to observe the transition to chaos, we shall study a much greater domain of the parameter space, without making a pretence of mathematical precision. Our main instrument is a one-dimensional return mapping, to which the Poincaré mapping, given by the phase flow close to the saddle, effectively reduces.

In the special case of mutually symmetric separatrices, a similar system was studied in [28, 29]. It was shown that chaos arises via a sequence of bifurcations reminescent of period-doubling, when two limit cycles merge into a pair of homoclinic loops of the saddle and generate twice as long a cycle; this transition is controlled by a single parameter. In the more general asymmetric case, the transition has to be described on a plane of two parameters, and the boundary of the domain of chaos appears to be fractal [30]. Some of the laws of similarity that arise here were recently discussed in [31].

In Section 2 the structure of the bifurcation diagram is indicated qualitatively, and we describe the recurrence process for "constructing" the lines bounding the domain in which only regular motions are possible. It is shown that this boundary includes a countable set of intervals, which correspond either to tangent bifurcation (transition to chaos via intermittency), or to a "boundary crisis" [32]. Close to all other points of the boundary, the bifurcation sequences are subject to universal laws of similarity; the points themselves divide into two sets with the power of a continuum, each with its own corresponding type of similarity.

The first type is similarity of the bifurcation structure of the successively imbedded domains on the plane of parameters. The imbedding sequences of different types are analyzed in Section 3 by means of the RG method.

The second type of similarity is analogous to the familiar scaling properties of critical circle maps [7, 8] and is studied in the next two sections. We show in the first that to the transition to chaos corresponds a family of fixed points of the renormalization transformation; contrary to the situation arising on a circle, the corresponding sequence of bifurcation parameter values oscillates while converging to its limiting values. In Section 5, where the structure of the domain of regular

behavior is considered, we show that, in addition to periodic motions, we encounter in it motions which are characterized by irrational rotation numbers and are analogous to stable motion over a cantorus surface [33]. When describing these latter modes we call them for brevity "quasi-periodic" (though strictly speaking this term is not entirely correct here). At the point of transition to chaos the cantorus converts into the analog of a two-dimensional torus. To this domain of parameter values there correspond singular fixed points of the RG transformations, which leads to super-exponential convergence of the bifurcation sequences.

Finally, in Section 6 we illustrate the previous sections by the results of numerical experiments with a system of ordinary differential equations, which models the averaged thermal convection in a rapidly oscillating gravitational field with weak violation of the inversion symmetry. The conclusions made above about the different types of similarity on the basis of analysis of discrete systems, are confirmed qualitatively and quantitatively.

One-dimensional return mapping can preserve or change the orientation of the intervals. In the sections mentioned, the case of orientation preservation is studied, since it seems to be more natural. In Section 7 we briefly describe the universal sequences of bifurcations that correspond to the cases of mappings which can change the interval orientation.

The homoclinic bifurcations dealt with in the present paper are not as strange an entity as that encountered in systems of ordinary differential equations. Besides, in the symmetric case the transition to chaos via homoclinic bifurcations is fixed, not only in finite-dimensional situations [28, 29], but also when studying numerically the distributed model, i.e., the complex Ginzburg–Landau equation [34]. This gives grounds for regarding the present class of systems as not exceptionally exotic and for expecting it to be possible to observe experimentally the transitions described below.

Return mapping

We take a system of n autonomous differential equations ($n \geqslant 3$), which, in the considered domain of parameter values, has the properties:

I) there is a saddle equilibrium state (point 0) for which there is a

one-dimensional unstable manifold (corresponding to the eigenvalue $\lambda_1 > 0$) and an $(n-1)$-dimensional stable manifold, corresponding to the eigenvalues $\lambda_2, \ldots, \lambda_n$, where $\mathrm{Re}(\lambda_n) \leqslant \ldots \leqslant \mathrm{Re}(\lambda_3) < \lambda_2 < 0$.

2) the two components of the unstable manifold (the one-dimensional separatrices Γ_1 and Γ_2) return to the neighborhood of the saddle 0, the return being on the same side of the plane stretched over the eigenvectors corresponding to $\lambda_1, \lambda_3, \lambda_4, \ldots, \lambda_n$, see Fig. 1. (The case when the separatrices return opposite to one another, i.e., on different sides of the plane, was considered by Turaev [35].)

To construct the mapping, we take an $(n-1)$-dimensional area A, close to the saddle, and transversal to the leading direction (given by the vector corresponding to λ_2). By the return of trajectories close to the separatrices, a mapping of this area into itself arises (Fig. 2), which can be written as a discrete relation connecting the coordinates of two successive intersections of trajectories with the area. The area is divided into two parts by $(n-2)$-dimensional "line" ϵ, on the different sides of which the trajectories leave the saddle zone along different separatrices. The mapping thus has a discontinuity at ϵ, and the trajectories starting on ϵ tend to the saddle point, since they belong to its stable manifold.

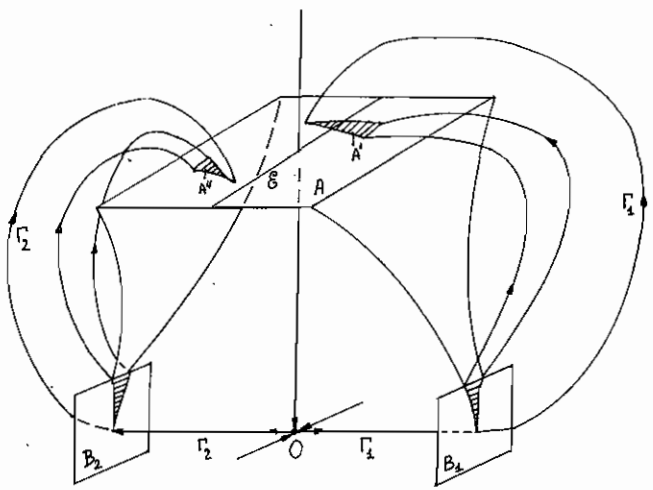

Figure 2 Poincaré mapping in area close to saddle point · Γ_1, Γ_2 are one-dimensional separatrices (components of unstable manifold of saddle point 0).
The scale of the figure is distorted: sizes are greatly reduced in the domains "outside" areas B_1, B_2.

The mapping $A \to A$ is best constructed as a composition of mappings $A \to (B_1 \cup B_2)$ and $B_i(B_2)$ into A, where $B_i (i = 1, 2)$ is an area close to the saddle and transversal to Γ_i. All the areas lie close enough to the saddle 0 for it to be possible to use linearization of the vector field about 0.

Since the real parts of the eigenvalues $\lambda_3, \ldots, \lambda_n$ are negative, there is strong compression along the corresponding directions. In the case of stable foliation at the area A, a one-dimensional mapping appears (in the appropriate coordinates) in the mapping. The image of the area A consists of a pair of narrow wedges A' and A'', stretched along the unstable direction. Thus the coordinate along this direction is the variable in the one-dimensional mapping. Close to the discontinuity this mapping has a singularity, which can be shown [36] to be determined by λ_1 and λ_2. In short, in the neighborhood of 0 the mapping has the form

$$x_{i+1} = F(x_i) = \begin{cases} F_+(x_i) = a_0(\mu) + (x_i)^z \cdot \varphi(x_i, \mu), & x_i > 0 \\ F_-(x_i) = b_0(\mu) + (-x_i)^z \cdot \Psi(x_i, \mu), & x_i < 0 \end{cases} \tag{1.1}$$

where the local coordinate x is measured along the unstable manifold, μ is the set of parameters, z is the saddle index:

$$z = -\frac{\lambda_2(\mu)}{\lambda_1(\mu)} \tag{1.2}$$

and the functions φ and Ψ are differentiable with respect to x.

Here, two cases can be distinguished (Fig. 3). With $z < 1$ (predominance of increasing mode) the derivatives at the point 0 are infinite, and we are concerned with the above-mentioned scenario, observed in the Lorenz system.

We shall consider the second case: $z > 1$, when the homoclinic loops are attractive, and the closed trajectories generated from them are stable, inasmuch as the mapping (1.1) has zero derivatives with respect to x at the point 0. We shall see that the transition to chaos takes place softly, via successive complication of the motion.

Depending on the form of functions $\Psi(x, \mu)$ and $\varphi(x, \mu)$, the mapping (1.1) may preserve or invert the orientation of intervals; at every point at which $F'(x) > 0$ ($F'(x) < 0$), the orientation of the

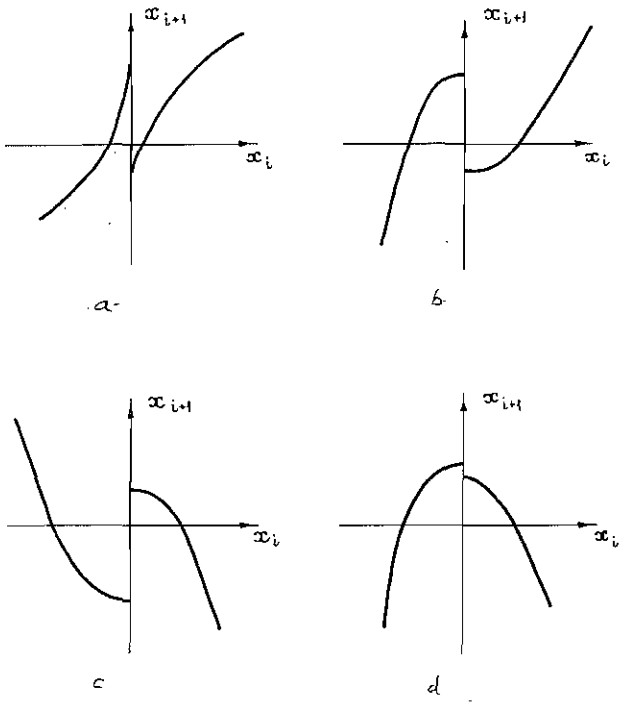

Figure 3 Forms of one-dimensional mappings near saddle
a) $\lambda_1 + \lambda_2 > 0$, orientable case
b) $\lambda_1 + \lambda_2 < 0$, orientable case
c) $\lambda_1 + \lambda_2 < 0$, non-orientable case
d) $\lambda_1 + \lambda_2 < 0$, semi-orientable case.

image of a small interval adjacent to this point is preserved (reversed). Generally speaking, the form of Ψ and φ is determined by the global properties of the phase flow remote from the saddle point. In the present paper we confine ourselves to the case when the functions $F_+(x)$ and $F_-(x)$ are strictly monotone in a sufficiently wide neighborhood of the point $x = 0$ (with $x \neq 0$). The orientation properties are then determined by the values of $\varphi(0, \mu)$ and $-\Psi(0, \mu)$, which are known as separatrix quantities [36]. It is assumed that these quantities do not change sign in the considered domain of parameter values.

The corresponding qualitative flow pictures are shown in Fig. 4; Fig. 4a refers to the positive separatric quantity $\varphi(0, \mu)$, and Fig. 4b to

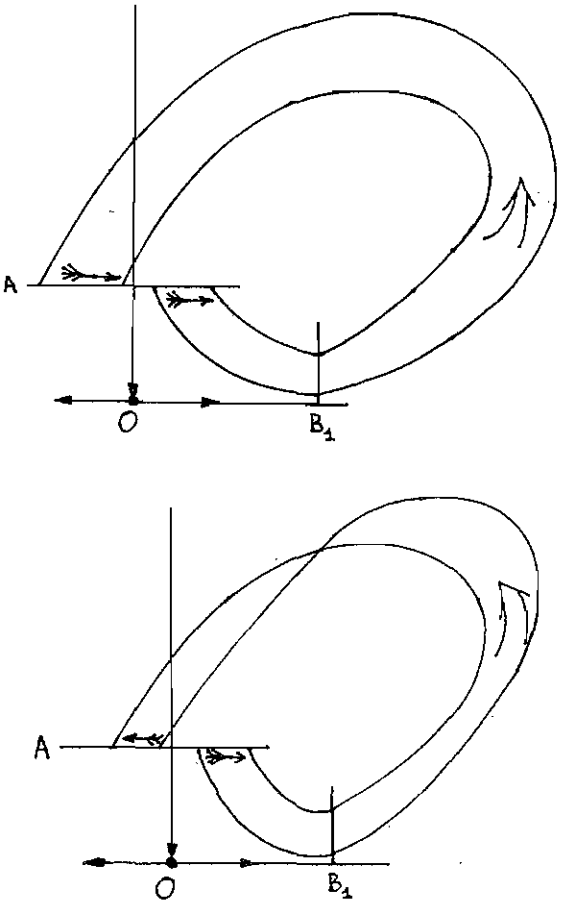

Figure 4 Property of orientability of sequence mapping
a) orientable case (preservation of interval orientation)
b) non-orientable case (change of interval orientation).

the negative. The situation when both separatrix quantities are positive, i.e., the return function increases on both branches (Fig. 3b), known as the orientable case, is analyzed in detail in Sections 2–6. The non-oriented case (Fig. 3c: negative separatrix quantities) and the semi-oriented case (Fig. 3d: separatrix quantities of opposite sign) are briefly outlined in Section 7.

Inasmuch as the one-dimensional mapping is regarded as a flow model, its properties are best described by using the terminology of continuous systems. The stable periodic point of the mapping, at which $F^m(x) = x$, will in fact be called an m-turn limit cycle (the corresponding attracting phase trajectory contains m turns before it closes).

As in continuous unimodal mappings of an interval, the sequence of iterations of the extremum fully characterizes the possible modes [37]; in piecewise monotone mappings of type (1.1), the definitive role is played by the two trajectories corresponding to one-dimensional separatrices of the saddle point 0, issuing into the domains $x > 0$ and $x < 0$; we shall call them the right Γ^+ and left Γ^- separatrices.

In a continuous system, situations are possible when one separatrix returns to the saddle, not after the first turn, but after several turns (and several returns to the secant area). Accordingly, satisfaction of the condition $F^{m-1}(F_+(0)) = 0$ (or $F^{m-1}(F_-(0)) = 0$) with $m > 1$ will henceforth be called the formation of an m-turn homoclinic loop, generated by the right (or left) separatrix.

The following analog of Singer's theorem [38] for continuous mappings can be proved: if, on both pieces ($x < 0$ and $x > 0$), the Schwartz derivative of the sequence function

$$Sf(x) = \frac{F'''(x)}{F'(x)} - \frac{3}{2}\left(\frac{F''(x)}{F'(x)}\right)^2 \tag{1.3}$$

is negative, and the mapping has a stable cycle, then at least one separatrix Γ^+ or Γ^- is attracted to it. Hence it follows at once that there cannot be more than two stable cycles in a mapping of this type for any parameter values.

Trajectories of the mapping are best coded by a sequence of symbols. Let the symbol "0" correspond to entry into the domain $x < 0$, and "1" to entry into $x > 0$. Then, corresponding to a periodic point we have a periodic sequence of symbols.

The coding will be denoted by digits in parentheses: e.g., P(0101) is a periodic point, $\Gamma^+(10, \ldots)$ is a right separatrix, etc.

To describe rearrangements that occur, it is useful to specify the concrete type of Poincaré mapping. Of course it then becomes a "model" mapping and is not the true mapping of return for a concrete system with a saddle point; on the other hand, as will be seen below, the families of such mappings behave in the same way when the parameters vary, i.e., we have universality. This means that we can confidently extend the results obtained when analyzing a comparatively simple discrete relation of the type (1.1) to continuous dynamic systems.

When choosing the family of mappings we have to preserve a number of parameters that is sufficient for adequately describing the observed sequences of bifurcations. This number can in fact only be established a posteriori; it is equal to the number of unstable eigenvalues in the spectrum of the fixed point of the corresponding renormalization transformation. It will be shown below that this number is two. Moreover, the model mapping must contain the saddle index z (in a physical problem it is generally a function of the external parameters, but we shall assume it to be a fixed constant). Starting from these considerations, in the oriented case it is convenient to take as the model the two-parameter family of mappings

$$x_{i+1} = F(x_i) = \begin{cases} F_+(x_i) = x_i^z - \mu_1, & x \geqslant 0 \\ F_-(x_i) = -(-x_i)^z + \mu_2, & x \leqslant 0. \end{cases} \tag{1.4}$$

With $\mu_1 = 0$ or $\mu_2 = 0$ the mapping (1.4) describes the case when one separatrix of the saddle point of a continuous system hits the stable manifold of the saddle, i.e., when a homoclinic loop is formed. The signs of μ_1 and μ_2 are chosen in such a way that, corresponding to positive values of them we get outwards breaking of the loop.

To pass to the semi-oriented case we have to change the sign ahead of the non-linear term in F_+, or in the non-oriented case, to change the sign in both F_+ and F_-.

2. ORIENTED CASE: QUALITATIVE DESCRIPTION OF SIMILARITY ON THE PLANE OF PARAMETERS

In this section we describe the main qualitative properties of a family of mappings (1.1) when the Poincaré mapping preserves the orientation both with $x > 0$ and $x < 0$, i.e., the sequence function is piecewise increasing. The corresponding quantitative analysis is given in later paragraphs with the aid of RG methods.

2.1. Basic types of bifurcations

In the present situation a stable periodic point (limit cycle) can appear or disappear in two general ways:

1) via a tangent bifurcation, when a stable and unstable cycle are born simultaneously and the eigenvalue of the linearization near the cycle is equal to $+1$;

2) via a homoclinic bifurcation, when the point $x = 0$ belongs to a cycle, i.e., the latter adheres to the loop of a separatrix.

Notice that, in the oriented case, period-doubling bifurcations are excluded from the families of mappings, since the eigenvalue of the linearization near a cycle is always non-negative ($F' \geqslant 0$) and cannot become -1.

Every typical bifurcation has co-dimension 1 and corresponds to a line on the plane of parameters. As regards the mutual disposition of the bifurcation curves, it can be seen at once that loop lines of the same separatrix with different symbolic codings cannot intersect transversally. Corresponding to the intersection of loop lines of different separatrices we have a point at which the saddle has a pair of doubly asymptotic trajectories with in general mutually asymmetric codings. From each such point a pencil of a countable number of homoclinic bifurcation curves departs; the pencil lies in the angle formed by two

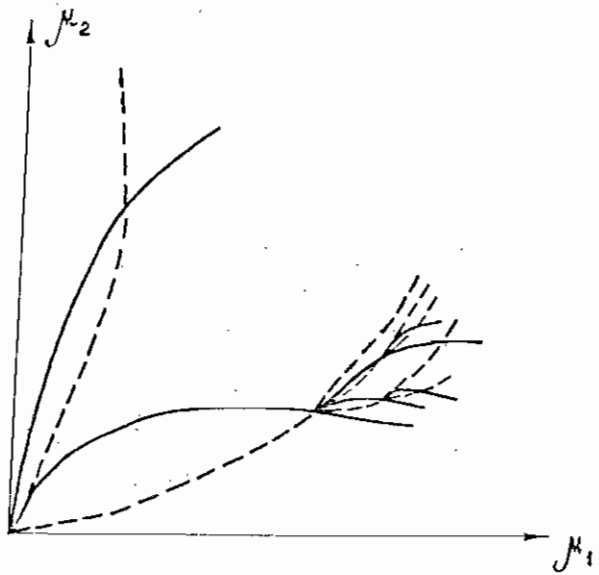

Figure 5 Intersection of lines of homoclinic bifurcations.

lines in which the two loops are broken outwards (Fig. 5, in which only homoclinic bifurcations are shown). On intersecting one another, lines of the pencil generate new pencils, and so on; it can be said that the domain around any point of intersection of lines of homoclinic bifurcations reproduces in miniature the entire bifurcation diagram.

2.2. *Domain of regular dynamics*

We shall start our description of "self-similarity" of a bifurcation structure and of the boundary of regular behavior with an analysis of the simplest possible motions admitted by the mapping (1.4). The fixed points are found from the equation $F_{\pm}(x) = x$. A pair "stable point — unstable point" is born when

$$\mu_1 = \mu*(\mu_2 = \mu*), \quad \mu* = (1 - z)\cdot z^{\frac{z}{1-z}} \tag{2.1}$$

(curves T_1 and T_2 of Fig. 6) and exists when $\mu* < \mu_{1,2} < 0$. When $\mu_{1,2} = 0$ the stable point disappears as a result of homoclinic bifurcation (these lines are denoted by $L_{1,2}$), while the unstable point exists for all positive values of the corresponding parameter $\mu_{1,2}$. With these unstable points P(0) and P(1) is connected a further phenomenon; the separatrix Γ^+ hits P(0) with

$$\mu_2 = \mu_1^z - \mu_1 \tag{2.2}$$

while Γ^- hits P(1) with

$$\mu_1 = \mu_2^z - \mu_2 \tag{2.3}$$

(curves C_1 and C_2 of Fig. 6). At the point of intersection of C_1 and C_2 the interval $(-\mu_1, \mu_2)$ doubles in length while mapping into itself, i.e., the mapping demonstrates chaos. Above C_1 a point of the domain $x \geqslant 0$ can depart to $-\infty$, while to the right of C_2 a point of the domain $x \leqslant 0$ can depart to $+\infty$. From the point of view of the modelled continuous system this departure signifies that the trajectory leaves the neighborhood of the saddle point and does not return to the secant area; the mapping cannot be used for analyzing attracting states. Thus, the curves T_1, T_2, C_1, C_2 bound a domain Q of non-trivial dynamics on the plane of parameters.

Let us now find the part of this domain in which the system behavior is certainly not chaotic, and the trajectories remain in the neighborhood

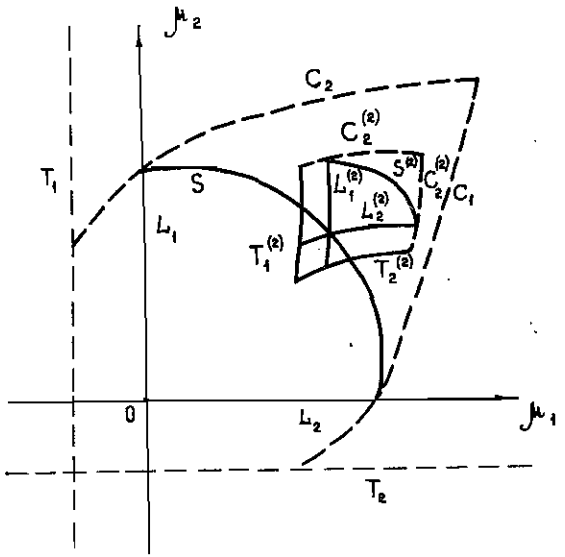

Figure 6 Bifurcation lines of simplest motions on parameter plane
L_1, L_2 are the lines of homoclinic bifurcations
T_1, T_2 are the lines of tangent bifurcations
C_1, C_2 are the lines of boundary crises
S is the critical line.

of the saddle. It naturally includes the parts of Q below $\mu_2 = 0$ or to the left of $\mu_1 = 0$, since there the mapping (1.4) is reversible. In the rest of Q a trajectory, whatever its starting-point, hits the interval $(-\mu_1, \mu_2)$ and remains there; it therefore suffices to consider the mapping of this interval into itself. We can distinguish a zone in which the mapping is invertible; it is bounded by the axes $\mu_{1,2}$ and by the curve S given by the relation

$$F_+(F_-(0)) = F_-(F_+(0)) \tag{2.4}$$

which we call the critical curve. For (1.4), the curve is given by the condition

$$\mu_2^z - \mu_1 = \mu_2 - \mu_1^z \quad (\mu_1 \geqslant 0,\ \mu_2 \geqslant 0) \tag{2.5}$$

which, with $z = 2$, defines the arc of a circle.

Deviation from the critical curve is characterized by the gap

$$\Delta = F_-(F_+(0)) - F_+(F_-(0)). \tag{2.6}$$

If the gap is absent ($\Delta = 0$), the mapping of $(-\mu_1, \mu_2)$ into itself is one-to-one. With a positive gap, the interval transforms into two, the sum of whose lengths is less than the length of the initial interval. In this domain, only regular motions are possible. With $\Delta < 0$, a piece arises where the mapping is not one-to-one, and in general, this can lead to chaos. Notice that, in the "subcritical" domain the curves of homoclinic trajectories cannot intersect: such intersection would contradict the uniqueness of the pre-image of every point (if a pre-image exists at all). On the other hand, the curves intersect the critical line in pairs: condition (2.4) implies the coalescence of separatrices after the second turn, and the closure of one into a loop must be accompanied by the formation of a loop from the other, the codings of these multi-turn loops being the same except for the first two terms (10 for Γ^+ and 01 for Γ^-). On the critical line, we have, for instance, pairwise intersection of the curves of homoclinic loops $\Gamma^+(100)$ and $\Gamma^-(010)$, $\Gamma^-(011)$ and $\Gamma^+(101)$, $\Gamma^+(1000)$ and $\Gamma^-(0100)$, etc.; on the axis of symmetry of the bifurcation diagram $\mu_1 = \mu_2$, the curves corresponding to formation of loops $\Gamma^+(10)$ and $\Gamma^-(01)$ pass through the critical line.

Thus the zone of regular behavior is certainly bounded by two pieces of curves T_1 and T_2 (tangent bifurcations), two pieces of curves C_1 and C_2 ("boundary crisis" — the trajectories cease to be localized inside the domain), and the critical line S. Notice that the line of boundary crisis joins C_1-smoothly (without a discontinuity of the first derivative) both with the critical line and with the lines of tangent bifurcations. We shall try to widen this non-chaotic zone.

We consider the double transformation F^2 (return mapping after two turns) in the domain above the μ_1 axis and to the right of the μ_2 axis. The central part of the graph of F(F(x)) has here the same form as the initial F(x) graph. We can therefore find for F^2 a pair of curves $T_{1,2}^{(2)}$ corresponding to the birth of two-turn cycles, lines $L_{1,2}^{(2)}$ of closure of two-turn homoclinic loops, curves $C_{1,2}^{(2)}$ on which one separatrix hits after two turns an unstable two-turn cycle, and a new "critical line" $S^{(2)}$ (defined by the condition $F_+^2(F_-^2(0)) = F_-^2(F_+^2(0))$, below which there can be no chaos (see Fig. 6). It was remarked above that the point of intersection of curves $L_1^{(2)}$ and $L_2^{(2)}$ belongs to the critical line S (with $\mu_1 = \mu_2$); consequently, a new zone of regular behavior, which lies around this point, intersects with the previous one. Thus, see Fig. 6,

"refinement" of the boundary of chaos amounts to a piece of critical line being replaced by convex "lobe," which consists of two further segments of lines of tangent bifurcations, two further segments of "boundary crisis" curves, and a new critical line.

It is easily shown that, for all $j \geqslant 2$, the curve of existence of a j-turn homoclinic loop of the separatrix Γ^+ intersects the critical line S. Through the point of intersection there obviously also passes the line of existence of the j-turn loop of separatrix Γ^+.

It can be shown that, close to the point of intersection of lines of j-turn homoclinic loops, the central piece of the F^j graph recalls the initial function F graph with a change of scale. Thus the piece of critical line S that passes through this point has to be replaced by a corresponding "lobe" (two lines of birth of j-turn cycles $T^{(j)}_{1,2}$ plus two lines of boundary crisis $C^{(j)}_{1,2}$ plus a critical line $S^{(j)}$).

For every $j > 2$ there are several such lobes, since different codings of the j-turn homoclinic loop are admissible (e.g., $\Gamma^+(100)$ and $\Gamma^+(101)$ with $j = 3$, $\Gamma^+(1000)$ and $\Gamma^+(1011)$ with $j = 4$, etc.). Of course, not all codings correspond to homoclinic bifurcations (e.g., there is no loop $\Gamma^+(1010)$), and not all loops are encountered on the critical line S, since the corresponding bifurcation curves may start, not at the point $\mu_1 = \mu_2 = 0$, but at a higher "secondary" point of intersection of the lines of homoclinic bifurcations (e.g., the line of loop 100011). To be more precise, adhering to the critical line are $j - W_j$ lobes, generated by j-loop structures, where W_j is the number of divisors of j.

After the domain of regular behavior has widened as a result of pieces of critical line S being replaced by lobes for all $j \geqslant 2$, almost nothing remains of the line S itself (we shall see in Section 4 that this "almost nothing" has non-zero fractal dimension). The boundary of the domain of regular behavior now consists of the residue of S, a countable number of intervals which correspond to tangent bifurcations, and to boundary crisis, and a countable number of new critical curves. But each of these new critical curves can similarly be built up, by replacing pieces of it by smaller second generation lobes (Fig. 7). An iterative process of refinement (or "building up") of the boundary of regular behavior is thus defined: at the first step, the basic zone, bounded by the lines T_1, T_2, C_1, C_2 and the critical line S, is constructed. At the second step, almost all this latter line is replaced by lobes, each of which includes its own critical line; at the next step, all these new critical lines are built up, and so on. Clearly, the result is a fractal curve [30, 31].

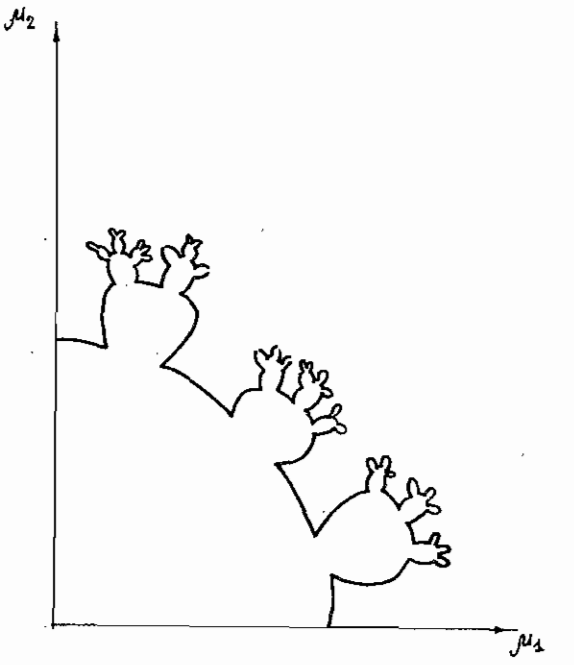

Figure 7 Refinement of boundary of domain of regular behavior.

Apart from the lines where cycles and boundary crises are born, the resulting "self-similarity" boundary includes residues of all the critical lines, and also a continuum of limit points, i.e., points at which the lobes accumulate as the number of tiers of them increases. Close to these points the bifurcation sequences behave in a universal manner. We shall describe this universality in more detail.

2.3. *Similarity of imbedded domains*

When constructing the "lobes" we have used the fact that, in a certain domain of parameter values, the j-th power of the return mapping is similar to the initial "one-turn" mapping F. In this domain, corresponding to bifurcation curves of the mapping there are similar curves for F^j, on which structures with j times the number of turns are transformed. Of course, this similarity holds, not only for the zone of regular behavior, but also for the domain of chaotic motions.

It was shown above that the domain Q of interesting dynamics on the $\mu_1\mu_2$ plane is bounded by the lines where the one-turn cycles (2.1) are born and the lines where the separatrices hit the unstable cycles (2.2) and (2.3). The lines $T_1^{(2)}$, $T_2^{(2)}$ shown in Fig. 6, where two-turn cycles are born, and the lines $C_1^{(2)}$, $C_2^{(2)}$ where separatrices hit after the second turn the unstable two-turn cycles, mark out on the parameter plane a domain $Q^{(2)}$, in which the dynamics of mapping F^2 are similar to the dynamics of mapping F in the larger domain Q.

On passing to cycles with other periods, these arguments can be repeated. Thus, for every $n \geqslant 2$ we obtain a domain $Q^{(n)}$, within which the properties of F^n are similar to those of F in Q. Consequently, within

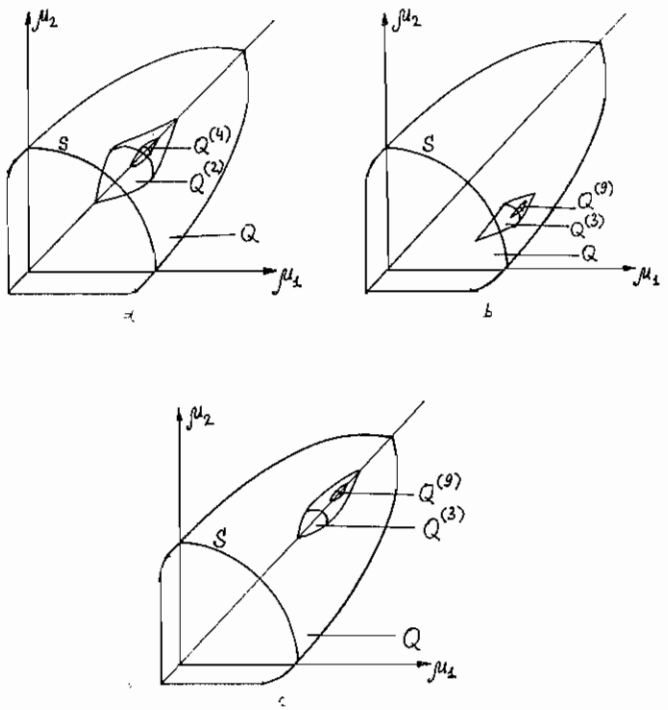

Figure 8 Sequences of imbedded domains on parameter plane
a) doubling
b) asymmetric tripling
c) symmetric tripling.

this domain is a smaller imbedded domain $Q^{(n^2)}$, where the mapping $F^{n^2}(x)$ reveals similar dynamics. On continuing this process, we obtain a system of similar domains imbedded inside each other.

The structure of the imbedded domains for $n = 2$ is shown in Fig. 8a. In this case all the bifurcation lines are symmetric under the replacement $\mu_1 \leftrightarrow \mu_2$, and as we move along the line $\mu_1 = \mu_2$ the entire system is cut along a diagonal. The similarity seen on this diagonal is very like Feigenbaum's [1, 2] and is described in detail in [29]. Specifically, the symmetric case implies that the bifurcations, are not generic, being a "Crisis of symmetry" of a stable cycle (with a pair of mutually symmetric cycles branching from it) and the "coalescence" of two cycles into one via the formation of a homoclinic figure of eight. Clearly, the "width" of the imbedded domains decreases faster than their "length", i.e., corresponding to deviation from the line of symmetry there is a supplementary scale of similarity, which can be found by the RG method (see [39] and Section 3.1 below), or by direct calculations for a concrete dynamic system (Section 6).

For every $n \geqslant 3$ the imbedding structure can be given in a different way, due to the existence (in different parts of the parameter plane) of cycles of the same length, but with different symbolic codings. In Fig. 8b we show the system of imbedded domains for the case, possible with $n = 3$, which corresponds to completely asymmetric motions.

It is now clear that the limit points to which the lobe sequences tend on accumulation when constructing the boundary of the domain of chaos, are the points to which the sequences of imbedded domains contract in the limit. Notice that it is not for every sequence that this point lies on the boundary of the basic (primary) domain of regular behavior (which contains the point $\mu_1 = \mu_2 = 0$). The necessary and sufficient condition for a point to belong to this boundary is that every successive imbedded domain intersect the critical line of the previous domain; for instance, for the symmetric sequence given by the relations

$$\begin{aligned} F_+^{(3)}(x) &= F_-F_-F_+(x) \\ F_-^{(3)}(x) &= F_+F_+F_-(x) \end{aligned} \tag{2.7}$$

this is not the case (Fig. 8c). Apart from the "basic" domain of regular behavior the parameter plane also contains a countable number of regular "windows," and a part of the points described belongs to their boundaries.

The class of considered structures can be widened by finding the

domains on the parameter plane in which $F^{m-1}F_+$ is similar to F_+, and $F^{n-1}F_-$ is similar to F_- with $m \neq n$. Obviously, the necessary and sufficient condition for the existence of such a structure is that two lines intersect on the plane, one corresponding to formation of an m-turn loop of a right separatrix and the other to an n-turn loop of a left separatrix. The limit points of such sequences clearly do not belong to the boundary of the primary domain of regular behavior.

2.4. *"Quasi-periodic" motions and the related universality*

Let us describe the motions observed in the domain of regular behavior. In view of the similarity of the lobes, it is sufficient to consider the domain of parameter values lying below the first critical line S, and the line itself.

With small positive μ_1 and μ_2 the derivative $F'(x)$ is everywhere small in the interval $[-\mu_1, \mu_2]$ and does not exceed unity, so that tangent bifurcations, for which the eigenvalue of the linearization near the cycle must become unity, are impossible. There are no unstable periodic solutions here, and there cannot be more than one stable solution (in which case all points of the interval without exception are attracted to this cycle). On the parameter plane the domain of existence of the stable m-turn cycle is bounded, on the one hand by the line, issuing from the origin, of formation of the m-turn loop of the right separatrix, and on the other hand, by the similar line for the left separatrix. These domains are shown in Fig. 9 for some simple cycles; the hatched parts refer to the presence of stable cycles.

On departure from the origin the graph of $F(x)$ near the edges of the interval $[-\mu_1, \mu_2]$ becomes steeper, so that tangent bifurcations become possible. Hysteresis is observed here, i.e., the co-existence of two stable cycles with the same number of turns. By tracing the evolution of a stable cycle as the parameters vary in this domain, we see that it is born from a homoclinic loop, and dies by merging with an unstable cycle via a tangent bifurcation (or vice versa, depending on the direction of motion). It can be seen from Fig. 9 that the two lines of tangent bifurcation (shown broken) join together at the point of "cusp." The unstable cycle exists everywhere inside the "angle" formed by these lines.

By extending the pair of curves of tangent bifurcation, we can see that they cut out a segment (arc AB of Fig. 9) on the critical line S; this

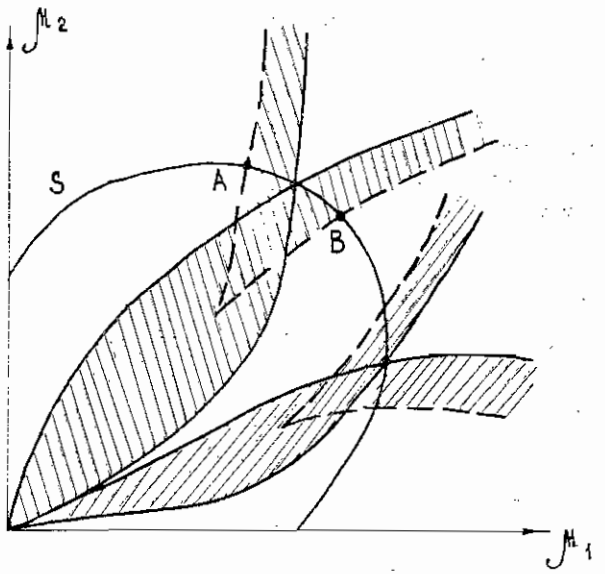

Figure 9 Domains of existence of stable cycles
—— are lines of homoclinic bifurcations;
- - - are lines of tangent bifurcations.

segment is easily seen to be the base of the lobe which is added to the main domain of regular behavior when its boundary is refined.

So as to order the periodic motions, and to see which further types of behavior are encountered in and on the boundary of the subcritical domain, we introduce characteristics from the point of view of which the mapping has a close resemblance to the familiar homeomorphisms of a circle.

In the present domain of parameter values, the images of all points of the real axis gradually enter the interval $[F_+(0), F_-(0)]$, and the interval maps into itself. Hence, on gluing together the ends of the interval, we get a mapping of the circle into itself, which defines all the limit motions of the initial dynamic system. At the point of gluing the mapping has a discontinuity whose width is equal to the gap (2.6), so that it does not reduce to a homeomorphism: when a gap is present each point of it has an image, but not each one has a pre-image. The rotation number ω can now be introduced in the usual way, by means of the lift of [40] or of the angle function [41]. To calculate ω, it is convenient to use the relation

$$\omega = \lim_{n\to\infty} \frac{S_n(x)}{n} \tag{2.8}$$

where $S_n(x)$ is the number of ones in the first n terms of the symbolic coding of the trajectory, starting at the point x. (The rotation number was introduced in a similar way for discontinuous mappings of an interval in [42–44].)

It can be shown by the standard methods that, with a non-negative gap, the limit (2.8) exists and is independent of the initial point x, and that rationality of ω is equivalent to the existence of a stable cycle (with $\omega = p/q$ the cycle consists of q points, p of which lie to the right of zero). It can also be shown that, in the zone of regular behavior, the rotation number depends continuously on the parameters; on moving through the first quadrant, it varies from zero on the axis of abscissae to unity on the axis of ordinates (at the point $\mu_1 = \mu_2 = 0$ it is not defined).

Obviously, in the initial continuous system, corresponding to a rotation number $\omega = p/q$ we have a closed q-turn phase trajectory, p turns of which lie to the right of the saddle, and $q - p$ turns to the left. The question naturally arises as to the structure of the motions to which irrational rotation numbers correspond.

For a start we consider the critical line S. Here there is no gap and no discontinuity, and the mapping (1.4) onto $(F_+(0), F_-(0))$ is a homeomorphism, strongly reminiscent of the familiar critical mapping of the circle into itself, of the form

$$x_{n+1} = x_n + \Omega - \frac{k}{2\pi}\sin(2\pi x_n) \tag{2.9}$$

which has been studied extensively, see e.g., [7, 8, 45]. But two essential differences should be noted. First, in the critical case $k = 1$ the mapping (2.9) has a cubic point of inflection, whereas the singularity in (1.4) is in general characterized by a non-integral exponent, namely, the saddle index z, which can take any positive values. Second, the sequence functions F_+ and F_- in (1.1) are not bound to be smoothly matched, since they are determined by the behavior of the trajectories in two different half-spaces. In particular, therefore, the derivative $F'(x)$ at the right end of the interval is in general not equal to the derivative at the left end, i.e., the mapping of the circle into itself is continuous but not smooth. Below, in Section 4, where we study the scale invariance of the bifurcation diagram in the neighborhood of S, we introduce a quantitative characteristic of this mismatch, which is an invariant of the corresponding RG transformation, which changes (as compared with (2.9)) the nature of the convergence of the bifurcation sequences and enables a supplementary family of universality classes to be distinguished.

At the qualitative level, the behavior of (1.4) on the critical line S is analogous to that of (2.9), which is familiar in dynamics. When the parameter varies along this line resonances are observed, i.e., stable cycles with all possible rational rotation numbers, and also "quasi-periodic" motions, which correspond to irrational rotation numbers. According to the general results of [40], the limit set for such a "quasi-periodic" mode is the entire interval $[F_+(0), F_-(0)]$; any trajectory is everywhere dense in it.

The dependence of the rotation number on the parameter (coordinate along the critical line) has a staircase type of graph, in which a step (interval of parameter values) corresponds to every rational ω. The stable cycle corresponding to a step disappears at its edges via a tangent bifurcation, while the piece of critical line corresponding to a step serves as base for one of the lobes added to the zone of regular behavior as its boundary is refined. The set of all parameter values corresponding to irrational ω has zero measure; below, in Section 4, we find numerically the fractal dimension of this set, which is not a universal constant (as in critical mappings (2.9) of the circle), but again depends on the saddle index z and the mismatch of functions F_+ and F_-.

Since the mappings (1.4) on S and (2.9) have qualitatively much in common, we can say that, at points of the critical curve corresponding to irrational ω, the attracting set of the initial continuous dynamic system is an object which is equivalent from the dynamical point of view to the rotation on a two-dimensional torus. Note that the geometrical configuration of this object is not associated with the usual ideas about a torus, but rather recalls the Lorenz attractor (see Fig. 10a); the phase trajectory densely fills a special kind of "tape", imbedded in three-dimensional space. The saddle point is a limit point of the trajectory, which thus returns again and again to the neighborhood of the saddle, coming indefinitely close to it. Thus the oscillogram of this motion has the form of relaxation oscillations with prolonged hovering about the equilibrium value (Fig. 10b).

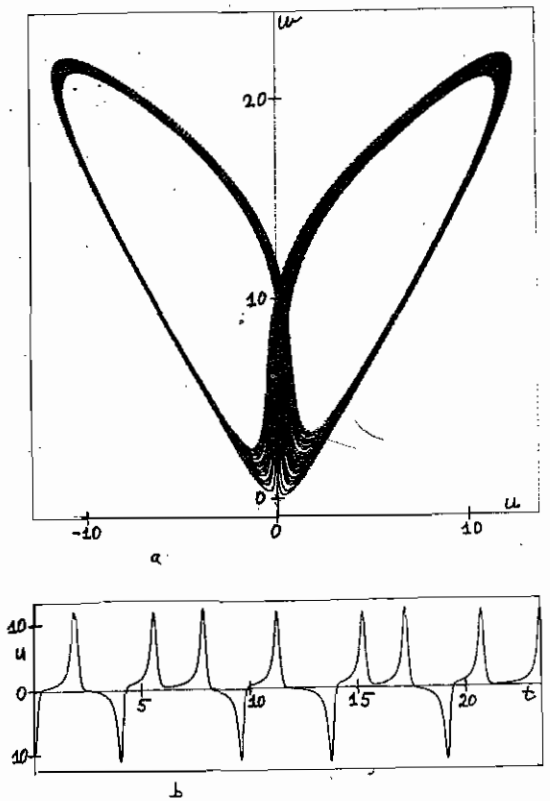

Figure 10 "Quasi-periodic" motion on critical line
a) two-dimensional projection
b) oscillogram.

In the same way as in theory of transition to chaos via a quasi-periodic mode [7, 8], close to irrational rotation numbers we observe similarity and scaling of the bifurcation sequences.

The qualitative picture is as follows. To be definite, we take the "golden mean" i.e., the rotation number $\sigma = \dfrac{\sqrt{5}-1}{2}$, whose continued fraction expansion consists of ones only. Its convergents are the ratios of Fibonacci numbers; 1/2, 2/3, 3/5, 5/8, etc. We depict the lobes for the cycles with these rotation numbers, calculated for (1.4). In

Fig. 11 we see that the domains of resonance accumulate at a point on the critical line, and their structures all have the similarity property: the picture of resonances transforms into itself if the scales across and along the critical line are varied by a suitable factor. This similarity is described quantitatively by the RG method treated in Section 4; the scaling scales are then obtained as the eigenvalues of the RG transformation linearized close to the fixed point, while the parameters of this transformation, which define the universality class, are the saddle index z and the mismatch of the return functions.

Let us see how the picture changes if we descend from the line S into the subcritical zone with positive gap (2.6). On moving "parallel" to the critical line, we encounter as before a countable number of resonance tongues and a continuum of "quasi-periodic" motions with irrational ω. No essential changes occur with the periodic states, except that, at the edges of a step, with large gaps (i.e., close to the origin

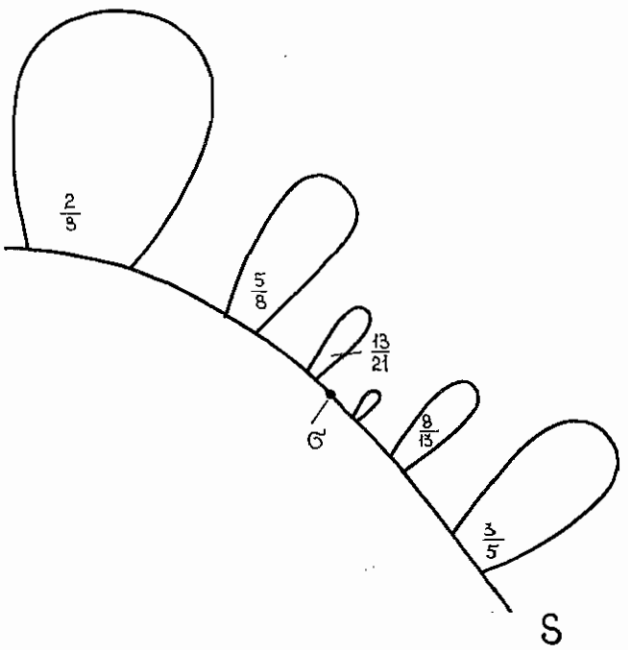

Figure 11 Scaling of "lobes" with rotation numbers approximating σ.

$\mu_1 = \mu_2 = 0$) they disappear, not via a tangent bifurcation, but by merging into a homoclinic loop. But the structure of the limit sets corresponding to "quasi-periodic" motions undergo substantial changes. It can be shown that, with any indefinitely small gap, the limit set cannot contain intervals; it is nowhere dense in the interval $[F_+(0), F_-(0)]$ and is a perfect Cantor set. (This recalls the familiar example of the diffeomorphism of a circle with irrational rotation number and the nowhere dense derived set constructed by Denjoy [46].)

In a continuous system the corresponding invariant attracting object is a special "Cantorus" (Fig. 12); as distinct from the Cantori familiar in conservative systems [33], it is stable. Points adjacent to it come closer in the course of time, till they hit the neighborhood of a saddle from different sides of its stable manifold. Like a "torus", this object is similar to a Lorenz attractor; as distinct from the "torus" the trajectories do not fill the "tape", but are attracted to a Cantor set in it. As

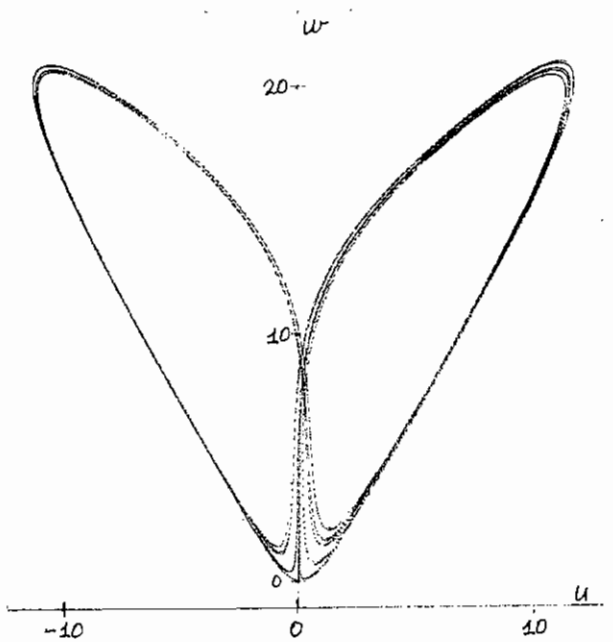

Figure 12 Two-dimensional projection of "Cantorus" in subcritical zone.

time passes, the ratio of the number of turns in the right half-space to the total number of turns tends to the irrational rotation number ω.

The quantitative characteristics of the bifurcation diagram are also essentially different on the curve S and in the subcritical zone bounding it. Lines corresponding to all irrational ω issue from the origin and cut S. Everywhere, the resonant tongues corresponding to suitable approximations to the irrational rotation numbers accumulate on the lines of these numbers. However, whereas on S itself the accumulation is according to the law of a geometric progression, when there is a gap (i.e., throughout the subcritical zone) the resonant domains converge much more rapidly towards σ. It will be seen in Section 5 that this is linked with the fact that, corresponding to the line S and the zone, with every ω, there are two distinct fixed points of the RG transformation; in the case of a mapping with a gap, the RG transformation has a singular fixed point (independent of the saddle index z).

Inside each lobe added to the basic zone of regular behavior, the regular modes can be ordered in the same way as in the basic zone, i.e., we can distinguish a countable number of periodic motions and a continuum of "quasi-periodic" motions. Of course, the rotation number has to be suitably redefined for each lobe: if it is based on a piece of S with rotation number p/q, then (2.8) gives p/q inside all the lobe, so that it has to be replaced by

$$\omega = \lim_{N \to \infty} \frac{\sum_{m=1}^{N} \sigma_{qm}(x)}{N} \tag{2.10}$$

where $\sigma_{qm}(x)$ is equal to unity if $F^{qm}(x) > 0$, and is equal to zero otherwise.

3. RG ANALYSIS OF SIMILARITY OF IMBEDDING

It was pointed out above that, inside each domain $Q^{(q)}$, based on the critical line on the resonance arc, corresponding to the rotation number p/q, the central part of the graph of $F^q(x)$ is similar to the graph of $F(x)$. It is therefore to be expected that the structure of the domain Q will be repeated in a reduced form in $Q^{(q)}$. A system of imbedded domains can therefore be considered on the parameter plane. In accordance with the

general ideas of applying the RG method to dynamical systems, we shall seek the mapping G for which F^q reduces to F by a linear change of scale. This G can be found for all numbers p/q in the interval (0, 1). As examples we take several of the simplest cases, then we obtain the explicit expressions for the scaling constants for any p/q with values of the saddle index z close to unity.

3.1. *Similarity of doubling type*

We find the transformation that formally converts a return mapping into a mapping after two returns. Since mappings with a discontinuity, defined by the two return functions F_+ and F_-, are being considered, G is most naturally introduced by means of a pair of functions:

$$G_z = \begin{cases} \eta(x), & x \geqslant 0 \\ \xi(x), & x \leqslant 0. \end{cases} \tag{3.1}$$

The behavior of the two functions close to the discontinuity is determined by the saddle index z, so that it is natural to consider the expansions

$$G_z = \begin{cases} \eta(x) = \sum_{j=0}^{\infty} a_j x^{jz} \\ \xi(x) = \sum_{j=0}^{\infty} b_j |x|^{jz}. \end{cases} \tag{3.2}$$

We take the normalization condition

$$\xi(0) = b_0 = 1. \tag{3.3}$$

In accordance with the form of F_+ and F_- (see (1.4)), the first coefficients of the series must satisfy the inequalities: $a_0 < 0$, $a_1 > 0$, $b_1 < 0$.

We consider the transformation after two units of discrete time (i.e., after two turns of the phase trajectory):

$$R(G_z) = \begin{cases} \alpha\xi\eta\left(\dfrac{x}{\alpha}\right), & x \geqslant 0 \\ \alpha\eta\xi\left(\dfrac{x}{\alpha}\right), & x \leqslant 0 \end{cases} \tag{3.4}$$

where the scale factor α is given by normalization condition (3.3):

$$\alpha = \frac{1}{\eta(1)}. \tag{3.5}$$

The passage from G_z to $R(G_z)$ is the required renormalization transformation. Its fixed point $T_* = (\eta_*, \xi_*)$ is given by the equations

$$\begin{pmatrix} \eta_*(x) \\ \xi_*(x) \end{pmatrix} = \begin{pmatrix} \alpha\xi_*\eta_*\left(\dfrac{x}{\alpha}\right) \\ \alpha\eta_*\xi_*\left(\dfrac{x}{\alpha}\right) \end{pmatrix}. \tag{3.6}$$

Transformation R is invariant under replacement of ξ by η and η by ξ. We shall therefore seek the symmetric fixed point for which $\eta_*(x) = -\xi_*(-x)$. Using this relation and introducing the function $g(x) = \eta_*(|x|)$, we can obtain the equation

$$g(x) = \alpha g g\left(\frac{x}{\alpha}\right) \tag{3.7}$$

which is the same as the Feigenbaum–Cvitanovic equation [1].

Transformation (3.4) can be linearized near the fixed point (η_*, ξ_*), then the eigenvalues and eigenvectors of the linear operator can be found. The eigenvalues with modulus exceeding unity define the scaling in the parameter space.

Clearly, perturbations near the fixed point can be divided into those that preserve and those that destroy symmetry. Accordingly, two groups of eigenvalues can be distinguished in the spectrum, one of which corresponds to perturbations belonging to the subspace of symmetric pairs of functions, and the other, to perturbations leaving this subspace.

The solution of system (3.6) with different z was sought numerically, by the method of polynomial approximation [1, 12]. Substitution in (3.6) of expansions (3.2) leads to a system of non-linear equations for the coefficients a_j and b_j. The roots of the equations are found by Newton's method. The eigenvalues of the renormalization transformation, linearized close to the fixed point, were approximated by the eigenvalues of the corresponding Jacobi matrix.

The results of calculations are shown in Fig. 13a. There are two eigenvalues with modulus exceeding unity. One (δ_1) corresponds to symmetry-preserving perturbations, and was found previously when

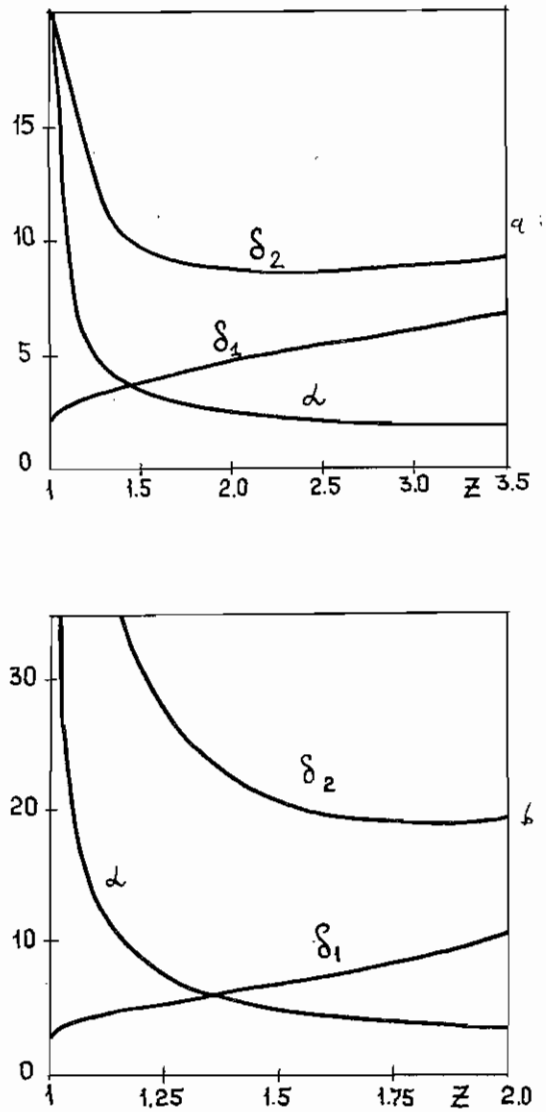

Figure 13 Dependence of scaling constants of similarity of imbedding on saddle index z.
a) doubling
b) asymmetric tripling.

analyzing systems with symmetric separatrices of the saddle. The other (δ_2) belongs to the part of the spectrum that describes symmetry-destructive perturbations. As distinct from δ_1, it does not depend monotonely on z, but reaches a minimum at $z = 2.2988...$ ($\delta_2^{\min} = 8.5397099...$). With $z = 2$ (quadratic singularity), $\alpha = 2.5029...$ and $\delta_1 = 4.6692...$ are the familiar Feigenbaum constants.

Accordingly, the structure of the imbedded domains of Fig. 8a transforms into itself when the scale along the axis of symmetry changes by a factor δ_1 and in the transverse direction, by a factor δ_2. For all values of z we have $\delta_1 < \alpha + \alpha^z < \delta_2$, so that, as the motions become more complicated, the "width" of the imbedded domains decreases much more rapidly than their "length", i.e., they stretch along the axis of symmetry.

3.2. *Different types of tripling*

The transformation of the return function after three turns can be analyzed in just the same way. For instance, for the structure of Fig. 8b we have to use the renormalization transformation

$$R\begin{pmatrix}\eta(x)\\ \xi(x)\end{pmatrix} = \begin{pmatrix}\alpha\xi\xi\eta\left(\dfrac{x}{\alpha}\right)\\ \alpha\eta\eta\xi\left(\dfrac{x}{\alpha}\right)\end{pmatrix}. \tag{3.8}$$

Calculations show that this transformation likewise has a fixed point for every $z > 1$, while there are two eigenvalues exceeding unity in the spectrum of the corresponding linearized operator. Here, as in the case of doublings, the fixed point is symmetric (its prototype for continuous mappings is well known, see e.g., [47]), so that these eigenvalues characterize the scaling on the parameter plane along the symmetric and asymmetric directions. Recall that the limit point to which the mutually imbedded domains contract does not belong in this case to the boundary of the basic (containing the point $\mu_1 = \mu_2 = 0$) zone of regular behavior.

When studying the properties of this boundary, we have to concern ourselves with the sequences of imbeddings which add to it new "lobes", i.e., with those with which are associated the rotation

numbers p/q. The sequence of triplings given by the rotation number 1/3 is shown in Fig.8b. This situation was considered in [48]. Here, the renormalization transformation is

$$R\begin{pmatrix}\eta(x)\\ \xi(x)\end{pmatrix} = \begin{pmatrix}\alpha\xi\xi\eta\left(\dfrac{x}{\alpha}\right)\\ \alpha\xi\eta\xi\left(\dfrac{x}{\alpha}\right)\end{pmatrix}. \tag{3.9}$$

There is now no symmetry between η and ξ, so that the fixed point is asymmetric. Calculations have shown that there is such a point for all $z \geqslant 1$; the two eigenvalues δ_1 and δ_2 greater than unity (Fig. 13b), indicating the change of scale on the parameter plane, do not correspond to perturbations with any sort of symmetry.

Obviously, the same constants are obtained if we analyze the sequence of triplings corresponding to rotation number 2/3 (the transformation is obtained from (3.9) if η is replaced by ξ, and ξ by η).

3.3. Similarity for any rational rotation number

We now describe the renormalization transformation corresponding to any rotation number p/q, where the integers p and q ($p < q$) have no common divisors. It has the form

$$R\begin{pmatrix}\eta(x)\\ \xi(x)\end{pmatrix} = \begin{pmatrix}\alpha\Psi_{p/q}\xi\eta\left(\dfrac{x}{\alpha}\right)\\ \alpha\Psi_{p/q}\eta\xi\left(\dfrac{x}{\alpha}\right)\end{pmatrix}. \tag{3.10}$$

The operator $\Psi_{p/q}$ is a $(q-2)$-tuple application of the function η or ξ; the function η is used $p-1$ times, and ξ is used $q-p-1$ times. The order in which ξ and η appear in $\Psi_{p/q}$ is uniquely determined by the number p/q. The factor α is found from the normalization condition, which in our case is (3.3).

When the saddle index is unity (piecewise linear mapping), the fixed point of (3.10) is

$$\eta(x) = x - \frac{q-p}{p}, \qquad \xi(x) = 1 + x. \tag{3.11}$$

For small $\epsilon = z - 1$ we can use expansion in ϵ (see [47] for this method as applied to continuous mappings of an interval). We shall consider the functions

$$\eta(x) = (1+a)x^{1+\epsilon} - \frac{q-p}{p} + d, \qquad \xi(x) = 1 - (1+b)|x|^{1+\epsilon}. \tag{3.12}$$

We assume that a, b, and d are small compared with unity. By using renormalization transformation we obtain a new pair of functions; for its coefficients a_R, b_R, and d_R, we have, up to higher order terms,

$$a_R = -\epsilon \ln\alpha + ap + b(q-p) + \epsilon(q-1) + \epsilon \ln\frac{(q-p)!p!}{p^q}$$

$$b_R = -\epsilon \ln\alpha + ap + b(q-p) + \epsilon(q-1) + \epsilon \ln\frac{(q-p-1)!p!}{p^{q-1}}$$

$$d_R = \frac{q-p}{p} + \alpha\left(pd + a\frac{p-1}{2} + b\frac{(p-q)(p-q+1)}{2p}\right) - \epsilon\alpha\left(\frac{q-p}{p}\ln\frac{q-p}{p} - \frac{\ln U}{p}\right) \tag{3.13}$$

where we use the notation

$$U = p^{q-2p}\cdot\frac{(p-1)^{p-1}\cdot(p-2)^{p-2}\cdot\ldots\cdot 2^2\cdot 1}{(q-p-1)^{q-p-1}\cdot(q-p-2)^{q-p-2}\cdot\ldots\cdot 2^2\cdot 1} \tag{3.14}$$

and the factor α is given by condition (3.3):

$$\alpha^{-1} = pd + a\frac{p+1}{2} - b\frac{(q-p)(q-p-1)}{2} + \frac{\epsilon}{p}\ln U. \tag{3.15}$$

On equating the new and old values of the coefficients, we find the values a_*, b_*, and d_*, corresponding to the fixed point. For instance, a_* is found from the relation

$$a_*(q-1) + \epsilon \ln a_* + \epsilon(q-1) + \epsilon \ln\frac{p!(q-p)!}{p^p(q-p)^{q-p}} = 0. \tag{3.16}$$

After calculating a_*, we find b_* and d_*:

$$b_* = a_* - \epsilon \ln \frac{q - p}{p}$$
$$d_* = - b_* \frac{(q-1)(2p-q)}{2p^2} + \epsilon \frac{p-1}{2p} \ln \frac{p}{q-p} - \frac{\epsilon}{p^2} \ln U. \quad (3.17)$$

Here, $\alpha_* = a_*^{-1}$, so that, on transforming (3.16), we obtain the relation connecting the scaling parameter α_* with the deviation ϵ of the saddle index from unity:

$$\epsilon = \frac{q-1}{\alpha_*} \cdot \frac{1}{\ln \alpha_* + (1-q) + \ln \frac{p^p (q-p)^{q-p}}{p!(q-p)!}}. \quad (3.18)$$

On linearizing the transformation (3.13) about the fixed point (3.16)–(3.17), we find the eigenvalues that define the scaling in the space of parameters, a, b, d. These eigenvalues are best expressed in terms of the factor α_*, which characterizes the scaling of the phase trajectory:

$$\delta_1 = q + \epsilon\alpha_* = q + \frac{q-1}{\ln \alpha_* + (q-1) + \ln \frac{p^p (q-p)^{q-p}}{p!(q-p)!}}$$
$$\delta_2 = q\alpha_*. \quad (3.19)$$

Up to discarded terms, the third eigenvalue is zero.

On substituting $q = 2$, $p = 1$, or $q = 3$, $p = 1$, in (3.18)–(3.19), we obtain the asymptotic expressions, given in [48] and [39], for the constants corresponding to "doubling" and "asymmetric tripling".

It can be seen from (3.18) that $\alpha_*(\epsilon)$ increases indefinitely as $\epsilon \to 0$, so that $\delta_1 \ll \delta_2$. It can also be seen that the two eigenvalues are mainly determined by the denominator q of the rotation number, the dependence on the numerator p being very weak. For instance, with $\epsilon = 0.001$, corresponding to the rotation number 1/7 we have $\delta_1 = 8.149$ and $\delta_2 = 8048.$, to 2/7 we have $\delta_1 = 8.191$ and $\delta_2 = 8340.$, and to 3/7 we have $\delta_1 = 8.208$ and $\delta_2 = 8454$.

It also follows from (3.18) that the same α_* (and hence the same δ) correspond to rotation numbers p/q and (q − p)/q. This is a consequence of the obvious symmetry: the fixed points of the RG transformations defined by these numbers transform into one another on changing the sign of the variable x.

The transition to chaos, connected with the fixed point of transformation (3.10), occurs as follows: from the "basic" zone of regular behavior, lying below the critical line S, the system moves through S and hits the lobe corresponding to rotation number p/q, then moves through the critical line of this lobe to hit the 2nd tier lobe corresponding to the same number p/q, etc.

Since (with small ϵ) we have $\delta_2 \gg \delta_1$, the lobes rapidly stretch out on transition along the direction corresponding to the lesser eigenvalue. On transition to a lobe of a subsequent tier the characteristic dimensions on the parameter plane decrease by a factor $g_{pq} \sim \delta_1^{-1}$. On summing g_{pq} over p and q, we can estimate the amount by which the total length of the critical lines of lobes added to the basic zone in the first step of refining its boundary exceeds the length of S. It can be seen from (3.17) that, as q increases, the factor α_* increases more slowly than q, so that $1/\delta_1$ drops no faster than 1/q. This gives grounds for assuming that, even after the first step, the "refined" boundary has infinite length (while embracing a domain of finite area on the parameter plane), i.e., the boundary is a fractal object and its dimensionality apparently exceeds unity.

The types of transitions here considered do not exhaust the entire set of limit points of sequences of imbeddings that belong to the boundary of the domain of regular behavior. For, in the domain where the central parts of the graphs of $F^m(x)$ and $F(x)$ are similar, given any integers j and m, we can indicate pieces on which the central part of the graph of $F^{jm}(x)$ is similar to the graph of $F^m(x)$. On the critical line of each lobe, therefore, regardless of its disposition, are based lobes of the next tier with all rational rotation numbers from 0 to 1. Thus the general form of the sequence of imbedded domains can be specified by the infinite numerical sequence p_1/q_1, p_2/q_2, . . ., p_j/q_j, . . ., where p_j/q_j is the rotation number corresponding to the step which we intersect on passing from the lobe of the j-th to the (j + 1)-th tier. The scaling properties obtained above refer only to a countable number of such sequences, namely, to those for which $p_1/q_1 = p_2/q_2 = \ldots = p_i/q_i = \ldots$. The entire set of sequences has the power of a continuum; it includes both periodic sequences (for which the generalization of the RG procedure is obvious), and aperiodic, "random" sequences. Every sequence has its own corresponding limit point on the parameter plane, and all these points belong to the boundary of the basic (including the origin) domain of regular behavior.

4. RG ANALYSIS OF NEIGHBORHOOD OF QUASI-PERIODIC MODES CLOSE TO THE CRITICAL LINE

In Section 2 we defined on the parameter plane the critical line S on which the return mapping is one-to-one. We also introduced a characteristic ω — the rotation number — which orders in a natural way the motions observed on this line. Here we shall describe the universal properties of systems close to S. The properties can be divided into two groups: local, which describe the similarity close to individual rotation numbers, and global, which characterize the organization of S as a whole. Below, we consider the local similarity near the rotation number equal to the "golden mean", then extend our results to the case of any irrational σ; and finally, we give data about the global characteristic, i.e., the dimension of the set of parameter values that correspond to irrational rotation numbers.

4.1. Golden mean

The golden mean, i.e., the number $\sigma = (\sqrt{5} - 1)/2$, is distinguished by the fact that its continuous fraction expansion consists of ones only: $\sigma = 1(1 + 1/(1 + \ldots))$; the best rational approximations of σ are the ratios Q_n/Q_{n+1} of the successive Fibonacci numbers; 2/3, 3/5, 5/8, etc.

We shall show that, close to S, the sequence of resonance domains corresponding to rational rotation numbers Q_n/Q_{n+1} convergent to σ, has similarity properties. Our approach is based on the RG method and is largely a repetition of the analysis in [7] for smooth mappings of a circle.

Let us describe the class of functions in which the renormalization transformation is constructed. Starting from the Poincaré mapping close to the saddle point, we consider pairs of functions $(\eta(x), \xi(x))$, having the properties;

1) $\eta(x)$ and $\xi(x)$ are defined respectively for $x \geqslant 0$ and $x \leqslant 0$, and are smooth functions of $|x|^z$:

$$\begin{aligned} \eta(x) &= a_0 + a_1 x^z + a_2 x^{2z} + \ldots \\ \xi(x) &= b_0 + b_1 |x|^z + b_2 |x|^{2z} + \ldots \end{aligned} \tag{4.1}$$

2) the normalization condition

$$\xi(0) - \eta(0) = 1. \tag{4.2}$$

The pairs of functions corresponding to the critical line S satisfy the matching condition (absence of a gap):

$$\eta\xi(0) = \xi\eta(0). \tag{4.3}$$

The renormalization transformation that realizes a shift of one step in the continued fraction (i.e., transforms one convergent approximation to the next) has the form [7]

$$R \begin{pmatrix} \xi(x) \\ \eta(x) \end{pmatrix} = \begin{pmatrix} \alpha\eta\left(\dfrac{x}{\alpha}\right) \\ \alpha\eta\xi\left(\dfrac{x}{\alpha}\right) \end{pmatrix} \tag{4.4}$$

where the factor α is given by condition (4.2):

$$\alpha = \frac{1}{\eta(0) - \eta\xi(0)} \tag{4.5}$$

(for the transformation to be realized we must have the inequalities $\xi(0) > 0$, $\eta\xi(0) > 0$, $\eta(0) < 0$).

It can be shown that transformation (4.4) leads to a dynamic system with a rotation number that varies according to the law: $\omega_R = 1/\omega - 1$; with $\omega = \sigma$ we have $\omega_R = \omega$.

As distinct from the smooth mapping of a circle [7, 8], in our problem the fixed point of transformation (4.4) does not in general fully characterize the situation; indeed, it may simply not exist. The point is that the two functions arising when the diffeomorphism of a circle is considered commute naturally with one another (i.e., $\eta\xi(x) = \xi\eta(-x)$). In our case this is certainly not the case, because F_+ and F_- are two distinct return functions. The mismatch of the pair (η, ξ) can be characterized quantitatively by the so-called break I:

$$I(\eta, \xi) = \frac{(\eta\xi(0))^{(z)}}{(\xi\eta(0))^{(z)}} = \frac{\eta'|_{\xi(0)} \cdot \xi^{(z)}(0)}{\xi'|_{\eta(0)} \cdot \eta^{(z)}(0)} \tag{4.6}$$

where the prime denotes differentiation with respect to x, and the superscript (z) denotes differentiation with respect to $|x|^z$. Obviously in the case of commuting η and ξ, the break $I(\eta, \xi) = I(\xi, \eta) = 1$.

Under transformation (4.4) the break I becomes its inverse:

$$I(R\eta, R\xi) = \frac{(\eta\xi\eta)^{(z)}(0)}{(\eta\eta\xi)^{(z)}(0)} = \frac{\eta'|_{\xi\eta(0)} \cdot \xi'|_{\eta(0)} \cdot \eta^{(z)}(0)}{\eta'|_{\eta\xi(0)} \cdot \eta'|_{\xi(0)} \cdot \xi^{(z)}(0)} = \frac{\xi'|_{\eta(0)} \cdot \eta^{(z)}(0)}{\eta'|_{\xi(0)} \cdot \xi^{(z)}(0)} =$$

$$= 1/I(\eta, \xi) \tag{4.7}$$

(we have used the matching condition (4.3)). Thus, if the break is not equal to unity, the transformation (4.4) cannot have a fixed point. If we now perform (4.4) again, the break returns to its initial value. (The scaling factor α_2 that appears at the second stage is not in general the same as the initial α_1.) Thus, from the point of view of the double transformation

$$R^2 \begin{pmatrix} \xi(x) \\ \eta(x) \end{pmatrix} = \begin{pmatrix} \alpha_1\alpha_2\eta\xi\left(\dfrac{x}{\alpha_1\alpha_2}\right) \\ \alpha_1\alpha_2\eta\xi\eta\left(\dfrac{x}{\alpha_1\alpha_2}\right) \end{pmatrix} \tag{4.8}$$

the break is a preserved quantity, like the saddle index z, i.e., is certain integral of the renormalization transformation. The transformation (4.8) converts the rotation number ω into $(2\omega - 1)/(1 - \omega)$. Multiple application of (4.8) causes no change of I: the space of pairs of functions is foliated into invariant surfaces, each with its own corresponding break value. Hence the fixed point of the double transformation has to be sought for each I.

The equations defining this point are

$$\xi_*(x) = \beta^2\eta_*\xi_*\left(\frac{x}{\beta^2}\right)$$

$$\eta_*(x) = \beta^2\eta_*\xi_*\eta_*\left(\frac{x}{\beta^2}\right) \tag{4.9}$$

where $\beta^2 = \alpha_1\alpha_2$.

With respect to transformation (4.4) the fixed point (4.9) is a cycle of period 2. Thus, if we consider the family of mappings with constant break, as we approach σ over consecutive continued fractions (and the corresponding resonance domains) we observe oscillations with period 2 of the corresponding similarity coefficients (similar oscillations of the similarity coefficients are noted in [49]). If the break is not fixed, and we consider e.g., the family (1.4) on the critical line, then, as we approach the parameter value corresponding to rotation number ω, the oscillating coefficients depart asymptotically to values corresponding to the break at the critical point.

To sum up, we can expect that the fixed points of transformation (4.8) will form a two-dimensional "manifold", the coordinates on which are the saddle index z and the break I. With fixed z, three typical groups can be distinguished in the spectrum of perturbations for each such point: perturbations which alter the break, those which destroy the matching condition (4.3), and finally, those which correspond to a shift of the rotation number.

It is immediately clear that perturbations which only alter the break are neutral, since the break of any perturbation (which satisfies (4.3)) and its image under (4.8) are the same. Obviously, therefore, the eigenvalue that characterizes these perturbations is unity.

Now take the perturbations which destroy condition (4.3), i.e., which lead to the formation of a gap (or overlap) and departure from the line S. If the gap is small, on iterations of transformation (4.8) it will increase exponentially:

$$\Delta_{R^2} = \beta^2 \cdot (\eta\xi\eta\xi\eta(0) - \eta\xi\eta\eta\xi(0)) \approx \beta^2 \cdot (\eta\xi\eta)'|_{\xi\eta(0)} \cdot (\xi\eta(0) - \eta\xi(0)) =$$
$$= \beta^2 \cdot (\eta\xi\eta)'|_{\xi\eta(0)} \cdot \Delta. \tag{4.10}$$

In order to find the quantity $(\eta_*\xi_*\eta_*)'|_{\xi_*\eta_*(0)} \equiv D$, we differentiate the relation obtained from (4.9):

$$\eta_*\xi_*(x) = \beta^2\eta_*\xi_*\eta_*\eta_*\xi_*\left(\frac{x}{\beta^2}\right) \tag{4.11}$$

with respect to $|x|^z$ at the point $x = 0$ and obtain $D = \beta^{2z-2}$, whence it follows that the eigenvalue characterizing perturbations which generate a gap, is β^{2z}; when (4.8) is applied, the gap (or overlap) is increased by a factor β^{2z}

Notice that there are eigenvalues of the type $\beta^{2z(1-j)}$ in the spectrum, which characterize the mismatch of the higher derivatives $(\eta\xi(0))^{(jz)}$ and $(\xi\eta(0))^{(jz)}$; this can be shown by slightly modifying the proof of Lemma 4.3 of [7]. These eigenvalues are less than unity and do not affect the critical dynamics of the mappings.

To find the eigenvalues corresponding to perturbations that shift the rotation number, we have to study numerically the spectrum of the renormalization transformation operator, linearized near the fixed point, i.e., we first have to find this point. Our method of solution is

based on polynomial expansion and is virtually the same as the method described in Section 3. It must be noted, however, that, on passing to finite segments of series (4.1), i.e., approximating the RG transformation, the break ceases to be invariant, while relation (4.3) is only satisfied approximately for the fixed points obtained (with an error that decreases with the order of approximation). For this reason, instead of projecting a continuum of fixed points onto the finite-dimensional subspace of parameters of this approximation, only a finite number of them is projected (the more, the more terms of the series are retained), so that a fixed point does not correspond to every value of the break. The criteria for the number of terms to be sufficient are that the spectrum contains an eigenvalue virtually equal to unity and another close to β^{2z}, and that the gap be small. Calculations show that, with $z - I \leqslant 1$ and moderate breaks, 10–12 terms are sufficient in the expansion of each of functions η and ξ in order for the equations $\lambda_1 = \beta^{2z}$, $\lambda_2 = 1$ and $\xi*\eta*(0) = \eta*\xi*(0)$ to be satisfied up to four–five decimal places.

In addition to this for all the fixed points thus found, there was a further eigenvalue greater than unity in the spectrum. This is λ_3, which corresponds to scaling of the space of parameters in reference to the change of rotation number.

Apart from fixed point calculations, a mapping of type (1.4) was used for studying similarities. Since the family (1.4) as such does not allow us to work with a constant break, we have to introduce a supplementary "neutral" parameter, such that the break can be fixed. In our numerical experiments we used the family

$$F(x) = \begin{cases} 1 + b|x|^z, & x \leqslant 0 \\ -a_0 + a_1 x^z, & x \geqslant 0. \end{cases} \tag{4.12}$$

Direct calculation from (4.6) shows that $I = (a_0)^{1-z}$. Condition (4.3) for the absence of a gap leads to the relation $1 + ba_0^z = a_1 - a_0$. As a result, one free parameter remains, variation of which causes a change of rotation number of the motion. We sought numerically the values of parameter b_n for which the point $x = 0$ belongs to the cycle with rotation number Q_n/Q_{n+1}, equal to the ratio of two successive Fibonacci numbers approximating σ (this corresponds to the appearance of a pair of homoclinic loops of the saddle in the continuous system). We then calculated the ratio of parameter increments

$$s_n = \frac{b_n - b_{n-1}}{b_{n+1} - b_n} \tag{4.13}$$

and the coefficients of the scale transformation

$$\alpha_n = \frac{F^{Q_{n-1}}(0) - F^{Q_n}(0)}{F^{Q_n}(0) - F^{Q_{n+1}}(0)}. \tag{4.14}$$

It can be seen from Table 1, which gives the results for $z = 2$ and $I = 0.I$, that, as n increases, s_n and α_n oscillate with period 2, while $\delta_n = \sqrt{s_{n-1}s_n}$ and $\beta_n = \sqrt{\alpha_n\alpha_{n-1}}$ tend to the constant values.

This behavior of s_n means that, on approaching σ, the width of the resonance domains corresponding to numbers approximating σ decreases in an oscillatory manner; while if we take a sequence of convergents approximating to σ only from one side (no matter whether from above or below), the width of the corresponding domains decreases according to the law of a geometric progression with ratio δ^{-2}.

Table 1

n	s_n	δ_n^2	α_n	β_n^2
5	−4.81184			
6	−2.25186	10.83561	−1.06222	1.41622
7	−2.45585	5.53024	−2.06554	2.54151
8	−3.24747	4.44233	−1.15029	1.73351
9	−2.21742	8.61134	−1.75452	2.17798
10	−3.45714	7.01177	−1.20289	1.88399
11	−2.17641	7.78641	−1.65091	2.04803
12	−3.49910	7.48761	−1.22594	1.94696
13	−2.16674	7.64449	−1.61786	2.00630
14	−3.50959	7.57259	−1.23488	1.97143
15	−2.16389	7.61298	−1.60702	1.99278
16	−3.51278	7.59162	−1.23821	1.98059
17	−2.16293	7.60412	−1.60335	1.98827
18	−3.51385	7.59699	−1.23941	1.98396
19	−2.16260	7.60124	−1.60208	1.98673
20	−3.51422	7.59988	−1.23986	1.98520
21	−2.16248	7.59945	−1.60164	1.98619
22	−3.51435	7.59934	−1.24002	1.98564

Calculations were made for different values of the saddle index z and the break I. As might be expected, the results are in good agreement with the data of numerical analysis of the fixed points of the

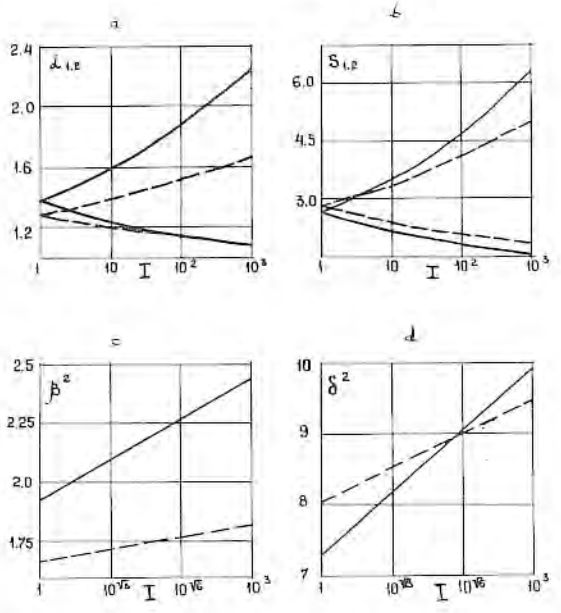

Figure 14 Dependence of scaling constants of similarity for $\omega = \sigma$ on the break I. — $z = 2$ — $z = 3$

renormalization transformation, while the values of the constants for the breaks I and I^{-1} are virtually the same (within the computational accuracy). In Fig. 14 we show the dependence of the similarity coefficients on the break (the abscissa is the "natural" coordinate ℓn I and not I itself). It can be seen that α and s vary quite strongly with the break; whereas β and δ, which characterize the scaling on approaching σ from one side, depend only weakly on the break. It is clear from Fig. 14, b, c, showing the dependences of β^2 and δ^2 on $\ell n^2 I$, that, in the entire range of examined values of the break (right up to 10^3), these dependences are graphically indistinguishable from straight lines.

4.2. *Arbitrary rotation number*

A similar analysis can be made for any irrational rotation number. Let the continued fraction expansion of the number be

$$\omega = \cfrac{1}{n_1 + \cfrac{1}{n_2 + \cfrac{1}{n_3 + \dots}}}. \tag{4.15}$$

Then, following [7], we find the renormalization transformation that corresponds to a one-step shift of the fraction:

$$R\begin{pmatrix}\xi(x)\\ \eta(x)\end{pmatrix} = \begin{pmatrix}\alpha\xi^{n_1-1}\eta\left(\dfrac{x}{\alpha}\right)\\ \alpha\xi^{n_1-1}\eta\xi\left(\dfrac{x}{\alpha}\right)\end{pmatrix} \tag{4.16}$$

where the factor α is defined as usual by the normalization conditions.

It is easily shown that, in the absence of a gap, the break $I(\eta, \xi)$ becomes its inverse under the action of this transformation, as in the case of the golden mean:

$$I(R\eta, R\xi) = \frac{(\xi^{n_1-1}\eta\xi^{n_1}\eta)^{(z)}(0)}{(\xi^{n_1-1}\eta\xi^{n_1-1}\eta\xi)^{(z)}(0)} = \frac{(\xi^{n_1-1}\eta\xi^{n_1-1})^{(z)}\big|_{\xi\eta(0)}\cdot(\xi\eta)^{(z)}(0)}{(\xi^{n_1-1}\eta\xi^{n_1-1})^{(z)}\big|_{\xi\eta(0)}\cdot(\eta\xi)^{(z)}(0)} =$$

$$= \frac{1}{I(\eta, \xi)}. \tag{4.17}$$

Thus, as in the case analyzed above, under the double transformation corresponding to a two-step shift of the continued fraction (conversion of the rotation number ω into $\omega/(1 - n_1\omega) - n_2$), the break is invariant. Hence, for every irrational ω, we obtain (with fixed z) a one-parameter family of universality classes, the coordinate in which is the break. Of course, in all classes of this family we have the same set, invariant under double transformation and defining the asymptotic dynamics of the system: it is a cycle if, for large k, the sequence $n_1, n_2, \dots, n_k, \dots$ is periodic (i.e., $n_k = n_{k+p}$; with $p = 1$ and $p = 2$ the cycle becomes a fixed point), or is a chaotic attractor if the continuous fraction expansion of the rotation number is not periodic [7, 50]. However, as distinct from problems that lead to smooth mappings of a circle, the quantitative characteristics of these cycles or attractors are not single constants for all systems, but are functions which depend continuously on the break (and also on z).

To sum up, at the qualitative level, the rearrangements that occur near S on transition to chaos are fully determined by the rotation number ω. For a quantitative description, as well as ω, it suffices to quote the saddle index and break corresponding to the point of transition, since, with fixed ω, z, and I, all systems behave in the same way.

4.3. Global properties of similarity

It was remarked above that the dependence of the rotation number on the critical line S on the coordinate along this line forms a typical "devil's staircase". A characteristic of this staircase is the dimension of the set of the parameter values that correspond to irrational rotation numbers, i.e., of the set which remains from the interval after discarding from it all the "steps" that correspond to rational numbers.

The fractal dimension D was calculated by the method given in [51], which is based on the construction of a hierarchy of steps by the "Farey tree" algorithm. At the first stage we find the pieces of critical line that correspond to the existence of cycles with rotation numbers $p_1/q_1 = 1/2$ and $p_2/q_2 = 2/3$. Then, in the interval between them, we find the arc corresponding to resonance with rotation number $p_3/q_3 = (p_1 + p_2)/(q_1 + q_2) = 3/5$. Two intervals between steps are thus obtained, and at the second stage we seek a step inside each of them (steps with rotation numbers $(p_1 + p_3)/(q_1 + q_3) = 4/7$ and $(p_3 + p_2)/(q_3 + q_2) = 5/8$ respectively). This process is continued so as to obtain at each new stage a step inside each interval, and after m stages the initial piece of critical line is divided into $2^m + 1$ steps with 2^m intervals between them. At each stage the dimension D is estimated from the relation

$$\sum_{j=1}^{2^m} (\ell_j)^D = L^D \tag{4.18}$$

where ℓ_j is the length of the j-th interval and L is the distance between the edges of the extreme right and left steps.

For calculating D we used the family of mappings (4.12), and the process of staircase construction was continued up to m = 9 (513 steps). The step edges, defined by the fact that tangent bifurcations occur on them, were sought by Newton's method. From the results of the previous section, it is to be expected that the dimension will depend on the break I. In Fig. 15 we show the curves D(I), obtained for z = 2 and z = 3. Obviously, $D(z, I) = D(z, I^{-1})$. The same values were obtained in numerical study of other families of mappings of this type; this gives grounds for assuming that, with fixed z, the break is the only parameter on which the dimension depends.

It must be said that, for families of mappings of type (1.4), in which the break is not fixed along the critical line, the fractal dimension is not

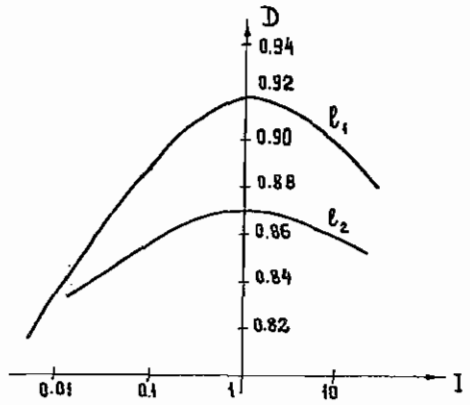

Figure 15 Dependence of dimension of devil's staircase on break I. ℓ_1 - z = 2; ℓ_2 - z = 3

a constant for the entire devil's staircase, but varies (along with I) as we move along it. Of course, this refers also to those situations in which the saddle index cannot be regarded as constant when the external "physical" parameters vary; here we need to speak of "local fractality" [52].

5. RESONANCES AND QUASI-PERIODIC MODES IN THE SUBCRITICAL DOMAIN

We saw from the qualitative discussion of Section 2 that the modes inside the domain bounded by the critical line S can be divided into periodic and "quasi-periodic". The structure of the subcritical domain differs from that of S, considered in the previous chapter. Below, we explain the reasons for this and consider the subcritical domain in more detail.

5.1. Properties of the limit set

The difference between the subcritical and critical cases can be explained qualitatively as follows. On the line S the segment $(F_+(0), F_-(0))$ maps into itself — the lengths of the image and preimage are the same. When a gap (2.6) is present, the mapping converts

the segment into two, of total length less than the initial length. Departure from the critical line and the appearance of a gap can thus be interpreted as the appearance of "dissipation". There is a similar situation when we consider period-doubling bifurcations: a crossover then appears, leading to the constants of the dissipative and conservative systems being different; the transition can be described by introducing into conservative mappings a small "dissipation" [53]. It will be shown below that the presence of "dissipation" in mappings of type (1.4) and (4.12) also leads to crossover, though the picture of similarity changes qualitatively: close to parameter values that correspond to irrational rotation numbers, the resonance domains corresponding to their approximating convergents accumulate as a super-exponential series, and not like a geometric progression (Section 4).

We pose the question of what happens to the invariant set in the interval when a gap is present, or in other words, what is left of the initial interval $(F_+(0), F_-(0))$ if we discard from it the gap and all its images under the action of F. The answer depends on the rotation number ω.

With rational $\omega = p/q$ and a small gap we have an unstable q-turn cycle, which co-exists with one or two such stable cycles. In the first case the invariant set consists of a countable number of intervals, and in the second, of q intervals, each bounded by points of stable cycles. If the gap is large enough, we saw in Section 2 that unstable cycles cannot exist, and the domain of existence of stability is bounded on the parameter plane by lines of homoclinic bifurcations. In this situation the invariant set is finite: it is exhausted by q points of a q-turn stable cycle.

If the rotation number ω is irrational, the invariant set is much more complicated. It obviously cannot be finite, since, if it were, the mapping would have a cycle. Let us state some claims about the limit set M (strict proofs can be made by the standard methods, see [40, 46], and Keener's paper [42]).

1. Every point belonging to M is the limit for a trajectory starting from any point of the interval $(F_+(0), F_-(0))$.

2. Between any two points of M an image of the gap lies, i.e., an interval $(F_-F_+(0), F_+F_-(0))$.

The gap and its images clearly cannot belong to the limit set. Hence the limit set contains no intervals. Its complement (the set of images of the gap) consists of intervals. Thus the set M is nowhere dense in the interval $(F_+(0), F_-(0))$ and is a perfect Cantor set.

3. Between any two points of M lies a pre-image of zero.

We need to dwell on this in rather more detail. Let the pre-image of zero (the point C) lie between points A and B belonging to M, and let it transform into zero: $F^j(C) = 0$, after j iterations of F. Thus, after j steps the images $F^j(A)$ and $F^j(B)$ of points A and B will be on different sides of zero, and after one more step, on different sides of the gap. In other words, no matter how close the points are to start with, after a certain number (possibly very large) of steps they will be a finite distance (of the order of the gap width) apart. This is the more curious in that, corresponding to a large size of gap, we have the situation when $F'(x) \ll 1$ throughout the interval, i.e., as the iterations proceed the images of points come closer and closer, till the next step takes them onto opposite sides of the gap. This dynamic behavior is similar to the behavior of Cherry flows on a two-dimensional torus [54, 55].

However, this fact gives no grounds for speaking of irregularity of the trajectory. Obviously, the kneading sequences [37] for mappings with the same irrational rotation number will be the same whether or not a gap is present, so that there is a semi-conjugacy between these situations, and the differences (though striking) are of a metric kind. We shall describe the crossover and the metric properties of the bifurcation sequence by taking the example of the golden mean σ, first for the case $z = 1$.

5.2. *Piecewise linear mapping*

We consider the mapping of an interval of unit length into itself:

$$F(x) = \begin{cases} a + bx, & a - 1 \leqslant x \leqslant 0 \\ a - 1 + bx, & 0 \leqslant x \leqslant a \end{cases} \tag{5.1}$$

where $0 \leqslant a \leqslant 1$. The critical line corresponds to the parameter value $b = 1$, while the gap width is $\Delta = 1 - b$.

We recall that the cycles are specified by a symbolic sequence $\{s_j\}$, where s_j is zero or unity, depending on whether the j-th point of the cycle is to the left or right of the point $x = 0$.

On the plane of parameters a and b, each resonance domain is bounded by lines corresponding to homoclinic bifurcations, i.e., to the points $x = a$ or $x = a - 1$ hitting the cycle.

It can be shown from (5.1) that the cycle specified by the sequence $\{s_j\}$, $j = 1, \ldots, n$, passes through $x = a - 1$ when

$$a = \bar{a}(b) = \frac{s_1 b^{n-1} + s_2 b^{n-2} + \ldots + s_n}{b^{n-1} + b^{n-2} + \ldots + 1}. \tag{5.2}$$

Knowing the symbolic sequences of the cycles corresponding to convergents approximating σ (they are easily found recurrently in terms of the Fibonacci numbers), we obtain from (5.2) recurrence relations for the consecutive values of the parameter $\bar{a}_n$ that correspond to these cycles:

$$\begin{aligned} \bar{a}_n &= \bar{a}_{n-1} \cdot b^{Q_{n-2}} \cdot \frac{1 - b^{Q_{n-1}}}{1 - b^{Q_n}} + \bar{a}_{n-2} \cdot \frac{1 - b^{Q_{n-2}}}{1 - b^{Q_n}}, \quad n \text{ even}, \\ \bar{a}_n &= \bar{a}_{n-1} \frac{1 - b^{Q_{n-1}}}{1 - b^{Q_n}} + \bar{a}_{n-2} b^{Q_{n-1}} \cdot \frac{1 - b^{Q_{n-2}}}{1 - b^{Q_n}}, \quad n \text{ odd}, \end{aligned} \tag{5.3}$$

where Q_n is the n-th Fibonacci number.

Similar expressions for the values of the parameter $\tilde{a}(b)$ that correspond to the other edge of the resonance zone with rotation number Q_{n-1}/Q_n, can be found by means of the relation

$$\tilde{a}_n = \bar{a}_n - (1 - b)^2 \frac{b^{Q_{n-2}}}{1 - b^{Q_n}}. \tag{5.4}$$

From (5.3) we obtain expressions for the ratios of increments of the bifurcation values of the parameter:

$$q_j = \frac{\bar{a}_{j-1} - \bar{a}_{j-2}}{\bar{a}_j - \bar{a}_{j-1}} = \begin{cases} -\dfrac{1 - b^{Q_j}}{1 - b^{Q_{j-2}}}, & j \text{ even} \\ -b^{-Q_{j-1}} \cdot \dfrac{1 - b^{Q_j}}{1 - b^{Q_{j-2}}}, & j \text{ odd}. \end{cases} \tag{5.5}$$

Expressions (5.5) describe the crossover. In the gapless case $b = 1$, noting that $Q_n \sim (1 + \sigma)^n$, we obtain $q_n \approx -(1 + \sigma)^2 = -(3 + \sqrt{5})/2$. For sufficiently large odd n, with $b < 1$, we have $q_n \simeq -b^{-(1+\sigma)^n}$, and for even n, the ratio $-q_n$ tends to unity.

Relation (5.4) shows that, as n increases, the width of the resonance domain corresponding to the n-th rational approximation of σ also decreases super-exponentially:

$$\bar{a}_n - \tilde{a}_n \simeq b^{(1+\sigma)^n} = b^{\left(\frac{3+\sqrt{5}}{2}\right)^n}. \tag{5.6}$$

5.3. *Singular fixed point of RG transformation*

In the general case $z \neq 1$, numerical data again reveal super-exponential convergence of the bifurcation sequence. If we assume that the ratio of increments of the bifurcation values of the parameter behaves according to the law

$$q_n \sim \exp(æ^n) \tag{5.7}$$

then the constant æ is the characteristic of this convergence. In calculations where the family of mappings (4.12) with a gap was studied, the dependence of this quantity on z was found (line ℓ_2 of Fig. 16).

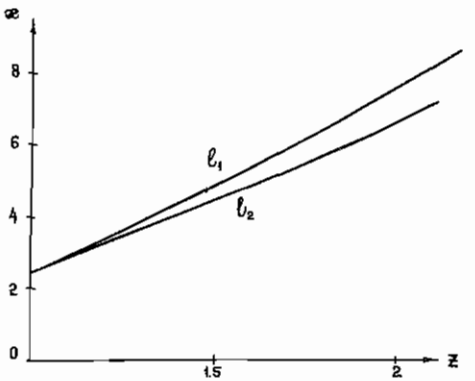

Figure 16 Dependence of rate of super-exponential convergence on saddle index z
ℓ_1 is dependence (5.14)
ℓ_2 are data of calculations for a family of mappings.

The constant of the super-exponential convergence can be found theoretically by using the RG method. For, it can be seen by inspecting the double transformation equation (4.9) that, apart from the above two-parameter family of "gapless" fixed points corresponding to the critical line, it admits a further fixed point, namely, the singular "step"

$$\begin{cases} \eta_*(x) = 0 \\ \xi_*(x) = 1 \end{cases} \tag{5.8}$$

(the scaling factor β is then infinite). This point is the same for all values of the saddle index. We write the original "initiating" perturbation about this point in the form

$$\eta(x) = -d + ax^z$$
$$\xi(x) = 1 - d - b|x|^z \tag{5.9}$$

where a, b, and d are small.

Successive application of transformation (4.8) does not change z, so that it can be expected that the quantitative aspects of the dynamics of systems which are close to the step (5.8), which is independent of z, will nevertheless be determined by z.

Substitution of the "initiator" (5.9) in transformation (4.8) leads (to a first approximation) to the following relations for the coefficients a_R, b_R, and d_R of the new pair of functions η_R and ξ_R:

$$a_R = z^{z+1}a^{z+1}b^z d^{z^2-1}$$
$$b_R = z^z a^z b^z d^{z^2-2} \tag{5.10}$$
$$d_R = \frac{a-d}{zabd^z}.$$

Consider the last relation. In general, its denominator is much smaller than the numerator, so that d_R is not small. The fixed point is singular, in that a small disturbance of it leads to the system being thrown a long way from its neighborhood. For the image of the initial disturbance to lie close to the point (5.8), the initiator must be in the neighborhood of its stable separatrix, i.e., with $a \approx d$.

The law of accumulation of the bifurcation surfaces corresponding to approximations to σ is determined by the rate of departure from the stable separatrix. We put $d = a + \varphi$, where φ is small compared with a and d; then,

$$\varphi_R = d_R - a_R \approx \frac{d}{za^{z+1}b}. \tag{5.11}$$

About the surface $a = d$ the RG equations (5.10) reduce to

$$a_R \approx a^{z^2+z}b^z$$
$$b_R \approx a^{z^2}b^z \tag{5.12}$$

and their solutions close to the fixed point $a = b = 0$ have the form

$$a_n \approx (a_0)^{æ^n}$$
$$b_n \approx (b_0)^{æ^n} \tag{5.13}$$

where the exponent æ of super-exponential convergence is found from the relation

$$æ = z + \frac{z^2 + \sqrt{z^4 + 4z^3}}{2}. \tag{5.14}$$

Clearly, the departure from the stable separatrix takes place in accordance with the same law

$$\varphi_n \approx \varphi_0 \cdot c^{æ^n - 1}, \quad c > 1. \tag{5.15}$$

In the linear case $z = 1$, æ is the same as the value given above by (5.6): $\sigma + 1 = (3 + \sqrt{5})/2$. With $z \gg 1$, the values given by (5.15) are in quite good agreement with the results of numerical study of the family of mappings (line ℓ_1 of Fig. 14).

Note finally that the singular step (5.8) and the displaced step $\eta(x) = -1$, $\xi(x) = 0$ characterize the dynamics for any irrational rotation number. For all such numbers the convergence of the bifurcation sequence is asymptotically of a super-exponential type; the quantitative aspects are determined by the continued fraction expansion of the number.

6. SEQUENCES OF BIFURCATIONS IN A SYSTEM OF DIFFERENTIAL EQUATIONS

We shall complement the above analysis of discrete systems by taking the case of similarity in successive homoclinic bifurcations for a continuous dynamic system; this case arises when analyzing the hydrodynamic problem.

The dynamics of the convective flow in a horizontal layer of viscous incompressible fluid, heated from below, and located in a rapidly oscillating vertical gravitational field, were considered in [56]. The basis of this work was the Lorenz system [14], in the first equation of which the term corresponding to the Archimedean force was multiplied by the modulation factor $\eta(1 + \cos \omega t)$, where ω is the dimensionless frequency of vibration, and η is the overload. The equations were reduced by the averaging method to the form

$$\dot{u} = P(v - u) + P \cdot D \cdot v(w - R)$$
$$\dot{v} = Ru - v - uw \tag{6.1}$$
$$\dot{w} = uv - bw.$$

The variables here are the (slowly varying) amplitudes of the basis functions in the Galerkin expansion of the stream function (u) and the temperature (v and w). The parameters P, R, and b have the same meaning as in the Lorenz model: P is the Prandtl number, b is a parameter defined by the wave number of the flow, and $R = Ra/Ra_0$ is the "normalized" Rayleigh number, i.e., the ratio of the Rayleigh number to its critical value (in the absence of modulation). The intensity of the vibrational action is characterized by the parameter $D = P \times \frac{1}{2} \times (\eta/\omega)^2$. It is to be expected that, with moderate D, the actual flow will be better modelled by system (6.1) than the ordinary thermal convection is modelled by the Lorenz system (in which (6.1) is converted with $D = 0$), since we know [57] that moderate vertical vibrations extinguish the small-scale convective disturbands that are ignored in the Lorenz approximation.

System (6.1) was studied in [29, 56]. We list the results of importance for our present study:

1) The system is dissipative, and the equations are invariant under the replacements $u \to -u$, $v \to -v$.

2) In the domain of parameter values $D < (R - 1)/R^2$ the trivial stationary solution $u = v = w = 0$, corresponding to mechanical equilibrium, is unstable and is a saddle with a one-dimensional unstable manifold.

3) With fixed $P = 10$ and $b = 8/3$ (which corresponds to the wave number of the most dangerous perturbations in the absence of vibrations) a line is discovered numerically on the plane of parameters RD, on which a pair of mutually symmetric homoclinic loops is formed in the phase space of the system, which are doubly asymptotic to the origin; on this line there is a point ($R = 12.79$, $D = 0.05$) to the right of which the saddle index

$$z = \frac{b}{-\frac{P+1}{2} + \sqrt{\left(\frac{P-1}{2}\right)^2 + P \cdot R \cdot (1 - DR)}} \qquad (6.2)$$

is greater than unity, and to the left of which it is less than unity. As R increases, corresponding to values of D less than 0.05 we have the Lorenz mechanism of transition to chaos [14, 23], while for larger D we have a different sequence of rearrangements, corresponding to the axis

of symmetry of Fig. 8a. The transition to chaos occurs here as the result of an infinite sequence of bifurcations, with each of which, as R increases, either the symmetric limit cycle gives up its stability to two asymmetric cycles branching from it, or else two mutually symmetric stable cycles merge into one homoclinic loop of a saddle which is twice the length. The sequence formed by the bifurcation values of the parameter converges with fixed values of the saddle index z according to the law of a geometric progression; the denominator of this progression is determined exclusively by the value of z, and up to the accuracy achieved with numerical integration of the system, is the same as the value predicted by the RG approach for the same z (the constant δ_1 of Section 3.1 above).

In order to study the general asymmetric case, we have to add to Equation (6.1) terms which destroy the invariance under the replacements of v by $-v$ and of u by $-u$. It can be expected that, when these terms are small, the separatrices of the saddle point will return to its neighborhood in the case of values of the parameters close to those at which the mutually symmetric separatrices of the undisturbed system return. Of course the symmetry of the equations (as in the initial hydrodynamic problem) can be infringed by a variety of methods; we choose the method which is simplest from the computational stand-point.

In Equations (6.1) the position of the saddle point does not depend on the parameter values, while the saddle index z is expressed in terms of these values by the explicit expression (6.2). By using (6.2), we can declare the saddle index to be a parameter, and relinquish one of the external, "physical" parameters by expressing it in terms of z. This means that we can move in the space of parameters with z fixed. We preserve these properties of the system while introducing into the third equation a phenomenological term au, where a is an "asymmetry parameter". Then, when $D < (R - 1)/R^2$, the point 0 is, as before, a saddle with a one-dimensional unstable manifold; in this domain the value of the saddle index is expressible by (6.2) in terms of the system parameters, and is independent of a (incidentally, this addition preserves for the system a specific property; for instance, a bifurcation that occurs on the boundary of the domain $D = (R - 1)/R^2$ is two-sided (it is not a generic case [41]); nevertheless, the events of interest to us, connected with homoclinic bifurcations, occur in a generic way). We replace the parameter D by its expression in terms of z obtained from (6.2).

To sum up, the object of numerical analysis is the system

$$\dot{u} = P(v - u) + v(w - R) \cdot \left[\frac{P}{R} - \frac{P}{R^2} - \frac{b}{R^2 z}\left(P + 1 + \frac{b}{z}\right)\right]$$

$$\dot{v} = Ru - v - uw$$

$$\dot{w} = uv - bw + au. \tag{6.3}$$

We fix the "traditional" parameter values P = 10 and b = 8/3; specifying values of the saddle index z, we shall study the qualitative and quantitative characteristics of the bifurcation diagram on the plane of the two remaining parameters R and a. Clearly, the line a = 0, corresponding to the undisturbed system (6.1), is the axis of symmetry of the diagram.

Equations (6.3) were integrated numerically by using Taylor expansion of variable order and recurrent calculation of the derivatives; the relative error per integration step, estimated by the last retained term of the series, did not exceed 10^{-10}. On the bifurcation diagram only the homoclinic bifurcations were traced, i.e., the lines on which there arise in the phase space of the system homoclinic loops of the right (issuing in the quadrant v > 0) or the left separatrix of the saddle. The results were divisible into three groups: the general type of bifurcation diagram (illustrations for Section 2), the data characterizing the scaling of the imbedded domains (Section 3), and finally, the results relevant to similarity of the structure of the parameter plane close to the lines of existence of "quasi-periodic" modes (Sections 4 and 5).

In Fig. 17 we show the bifurcation diagram of system (6.3) with z = 1.5. The lines A and B refer to the simplest one-turn homoclinic loops of the saddle (with codings 1 and 0 respectively), while from their point of intersection issues a pencil of bifurcation curves. The lines of the pencil corresponding to relatively simple loops (with only a few turns) are numbered at the upper edge of Fig. 17; the numbers refer to the following loop coding:

1 — ABAAA,	2 — BAAAA,	3 — ABAA,	4 — BAAA,
5 — ABA,	6 — ABB,	7 — AB,	
8 — BA,	9 — BAA,	10 — BAB,	
11 — ABBB,	12 — BABB,	13 — ABBBB,	14 — BABBB,

(6.4)

where the letter A denotes unity and B denotes zero. It can be seen that, as might be expected, the lines of loops whose codings differ by only the first two symbols, intersect on the critical line S; below these line there are no intersections.

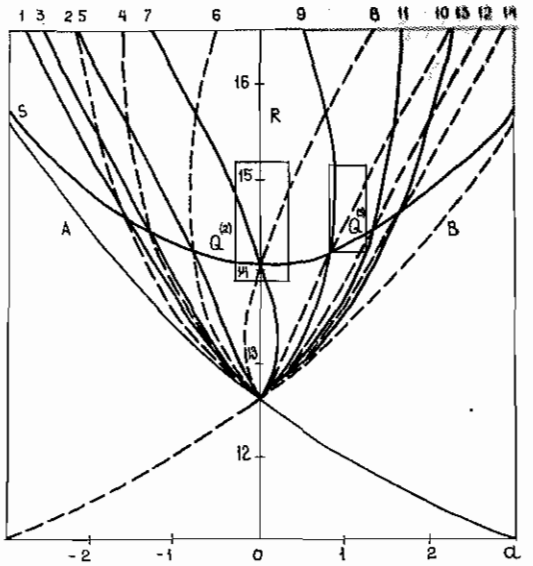

Figure 17 Bifurcation diagram of Eqs. (6.3); lines of simplest homoclinic bifurcations.

As was conjectured in Section 2, new pencils issue from the points of intersection of lines of homoclinic bifurcations, etc. The domain bordering the point of intersection of the lines of homoclinic loops with codings 10 and 01 (in Fig. 17 it is enclosed by the rectangle $Q^{(2)}$) is shown on an enlarged scale in Fig. 18, where the stretching along the horizontal is greater than along the vertical. We see from Fig. 18 that it has roughly the same structure as the bifurcation diagram as a whole. The bifurcation curves shown here correspond in order of numbering to the homoclinic loops with codings (6.4), but now A denotes the pair of symbols 10, and B denotes 01. Again, the lines of loops whose codings differ by the first two symbols (which now corresponds to four turns of a separatrix) intersect in pairs on the critical line $S^{(2)}$.

The region around the intersection point of lines of 4-turn loops (rectangle $Q^{(4)}$ in Fig. 18) is given in Fig. 19. The curves again denote loops with codings (6.4) but A and B now stand for 4-turn elements 1001 and 0110. We see that the structure of this part of the diagram reproduces that of the larger domain $Q^{(2)}$ in which it is imbedded.

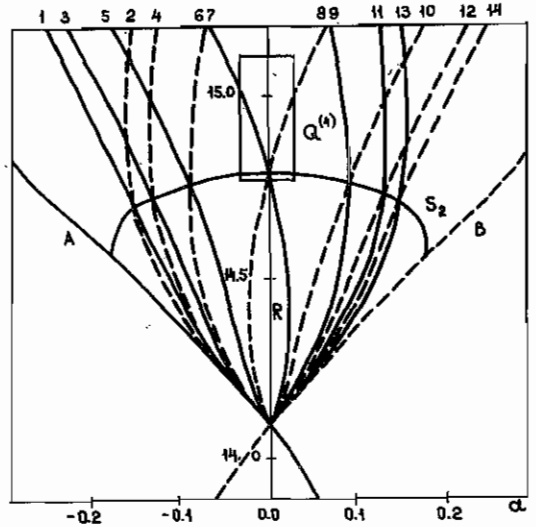

Figure 18 Domain of parameter plane around point of intersection of lines of appearance of two-turn homoclinic loops (enlarged rectange $Q^{(2)}$ of Fig. 17).

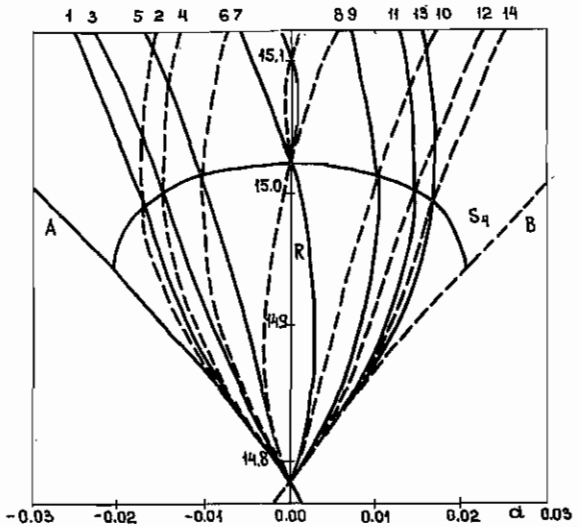

Figure 19 Domain of parameter plane around point of intersection of lines of appearance of four-turn homoclinic loops (enlarged rectangle $Q^{(4)}$ of Fig. 18).

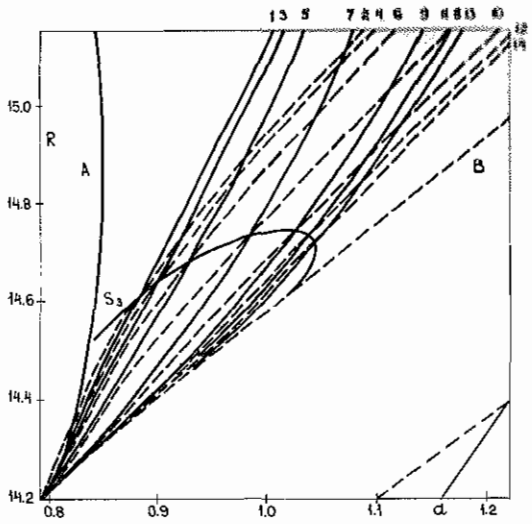

Figure 20 Bifurcation lines near point of intersection of lines of formation of three-turn homoclinic loops (enlarged rectangle $Q^{(3)}$ of Fig. 17).

The points of intersection of the bifurcation lines about which these enlarged domains are located lie on the axis of symmetry of the diagram and correspond to the sequence of imbeddings given by the rotation number 1/2. In Fig. 17 the domain $Q^{(3)}$, which does not cut the axis of symmetry, contains the point of intersection of the lines where loops arise with codings 100 and 010 (this point lies on the segment of the critical line S that corresponds to the rotation number 1/3). The lines shown in Figure 20 also refer to homoclinic bifurcations with codings (6.4), but now the "elementary structures" are three-turn: A denotes 100 and B denotes 010. To sum up, for the system of equations (6.3) the conclusion based on the analysis of mappings has been fully confirmed, that the bifurcation diagram as a whole is qualitatively similar to the individual pieces of it close to the points of intersection of homoclinic bifurcations. We now turn to the quantitative aspects of the similarity.

Among the various possible sequences of imbedded domains on the parameter plane, we confine ourselves to the "doubling" sequence, corresponding to rotation number 1/2. Since this sequence includes the axis of symmetry, the calculations are simplified, and we can study quantitatively the longitudinal (corresponding to the lesser of constants $\delta_{1,2}$) as well as the transverse scaling. We show the lines of 2^n-turn

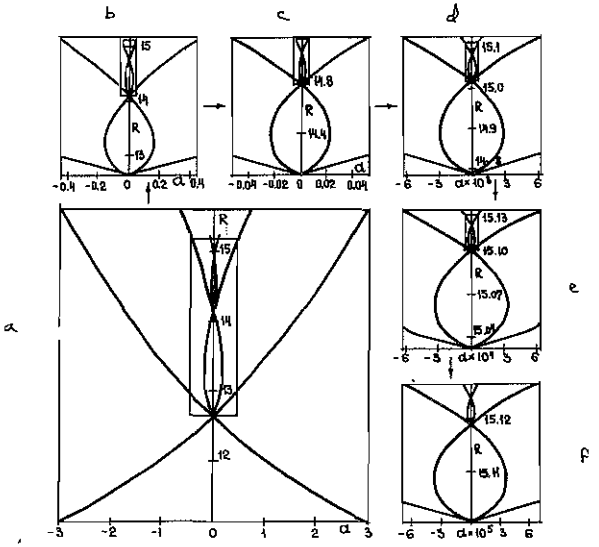

Figure 21 Similarity of imbedding on parameter plane for system (6.3); lines of appearance of 2^n-turn homoclinic loops.

loops. In Fig. 21a we show the domain around the point of intersection of the one-turn loops with z = 1.5. From this point issue two lines, corresponding to loops with codings 10 and 01; from the point of intersection of the lines of these two-turn loops issue lines of four-turn loops 1001 and 0110, which in turn intersect, etc. Each of Figs. 21a–f contains a rectangle bounding the domain around the point of intersection of two bifurcation lines, while the next Figure shows the transformation of this rectangle into an enlarged square. The last two Figures are quantitatively almost the same (the sequence was taken up to 64-turn loops), and we can measure directly the scaling factors in the parameter space, along and across the axis of symmetry. For more accurate calculation we write the ratios

$$\delta_1^{(n)} = \frac{R_{n-1} - R_{n-2}}{R_n - R_{n-1}} \tag{6.5}$$

where R_n is the R coordinate of the point of intersection of the lines of 2^n-turn loops (this point lies on the a = 0 axis, so that it was actually calculated for system (6.1), see [29]). In Table 2 we quote $\delta_1^{(n)}$ for several z; clearly, they tend to the values $\delta_1^{(RG)}$ quoted in the last column and obtained by RG analysis in Section 3.

Table 2

z	$\delta_1^{(5)}$	$\delta_1^{(6)}$	$\delta_1^{(7)}$	$\delta_1^{(8)}$	$\delta_1^{(RG)}$
9/8	2.86629	2.91612	2.91759	2.91668	2.91394
5/4	3.20221	3.24190	3.25657	3.23593	3.25961
4/3	3.38674	3.43512	3.44793	3.45379	3.45446
3/2	3.70835	3.77570	3.79401	3.79824	3.80056
5/3	3.98973	4.07990	4.10352	4.10813	4.11099
2	4.47595	4.62114	4.65837	4.66568	4.66920
5/2	5.07856	5.32558	5.39226	5.40638	5.41274

The transverse scaling is given e.g., by the relation

$$\delta_2^{(n)} = \frac{a_{n-1}}{a_n} \tag{6.6}$$

where a_n is the a coordinate of the point on the line where the 2^n-turn loop arises with $R = (R_{n-1} + R_n)/2$. The corresponding sequences $\delta_2^{(n)}(z)$ are given in Table 3; the penultimate column shows the ratio for the lines of 64- and 128-turn loops.

Table 3

z	$\delta_2^{(3)}$	$\delta_2^{(4)}$	$\delta_2^{(5)}$	$\delta_2^{(6)}$	$\delta_2^{(RG)}$
9/8	14.15827	15.28692	15.64498	15.60283	16.2208
5/4	10.34678	11.23832	11.56855	11.66726	12.0307
3/2	7.83801	8.82868	9.26203	9.39645	9.6694

Since the transverse size decreases much faster than the longitudinal, the error of these ratios is greater than in the case of longitudinal scaling, so that the calculated values are not in as good agreement with the values of $\delta_2^{(RG)}$, obtained in Section 3.1 and shown in the last column.

We now consider the structure of the bifurcation diagram of system (6.3) near the lines where "quasi-periodic" motions exist. Here, the results of RG analysis (Sections 4, 5) predict exponential scaling of the resonance domains near the critical line S, and super-exponential scaling in the subcritical zone. As above, we chose for calculations the golden mean, i.e., the rotation number $\sigma = (\sqrt{5} - 1)/2$. In Fig. 22a we show the line $a_\sigma(R)$, corresponding to this mode with z = 1.5; convergent to it is the sequence of lines of 2-, 3-, 5-, etc. turn loops of the two saddle separatrices, which have Fibonacci symbolic coding (only the lines of loops of the right separatrix are shown in Fig. 22a).

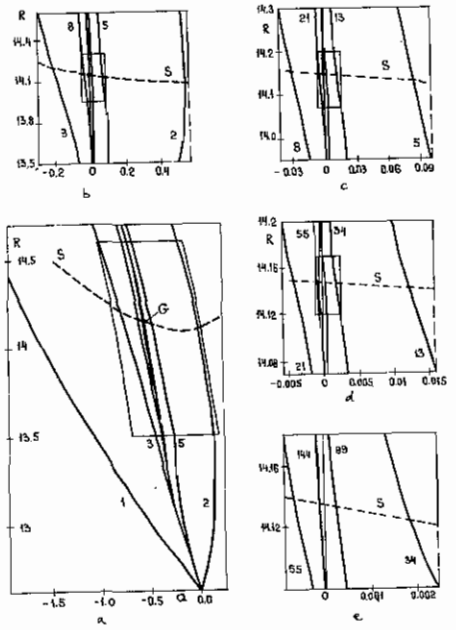

Figure 22 Similarity close to critical line S for Eqs. (6.3): lines of homoclinic loops corresponding to rotation numbers approximating σ.

In the subcritical zone these lines condense very rapidly. The distance between the curves falls catastrophically as the motion becomes more complex, and the further below the critical line, the less it is possible to distinguish between the curves (with machine accuracy). For different R we obtained the sequences $\{a_n(R)\}$, corresponding to these loops, and the convergence was characterized by the quantity

$$æ_n = \frac{\ell n \dfrac{a_n - a_{n-1}}{a_{n-1} - a_{n-2}}}{\ell n \dfrac{a_{n-1} - a_{n-2}}{a_{n-2} - a_{n-3}}} \tag{6.7}$$

which is the rate of exponential scaling (n is the number of the Fibonacci number Q_n). Unfortunately, due to their rapid "collapse", the sequences are too short to have time to reach asymptotic behavior. For instance, with R = 12.7, we can distinguish from the pencil the line of

formation of the 34-turn loop (at a distance $\Delta a \approx 1.16 \times 10^{-11}$ from the line of the 21-turn loop) and $æ_9 = 4.31$ (the approximate RG theory of Section 5 predicts for z = 1.5, in accordance with (5.14), the value æ = 4.78). As R increases, the departure to asymptotic behavior slows down and $æ_9$ decreases. But even with R = 13.3, it is possible to distinguish from the line of the 34-turn loop the lines of the 55- and 89-turn loops, where $æ_{11} \approx 4.21$.

The closer to the critical line, the higher the resonances at which crossover occurs, while ordinary scaling is observed for relatively simple structures with only a few turns. The structure of the parameter plane is almost exactly reproduced on passing to higher resonances (with transformation of the rotation number according to the law $\omega \to (\omega + 1)/(\omega + 2)$) and at the same time different changes of scale along and across the critical line S; the center is the point G, at the intersection of S and $a_\sigma(R)$. Each diagram in Fig. 22, starting with the second, is an enlargement of a fragment of the previous diagram, and their similarity is obvious. The number of turns in a loop is shown next to each line.

Extra calculations were made to find the factor indicating the change of scale along S. In Table 4 we show the ratios of increments of the parameters of sequence $\{\tilde{a}_n\}$, where $\tilde{a}_n$ is the a coordinate of the point of intersection of S and the line of formation of the Q_n-turn loop. The quantity

$$s_n = \frac{\tilde{a}_{n-1} - \tilde{a}_{n-2}}{\tilde{a}_n - \tilde{a}_{n-1}} \tag{6.8}$$

clearly oscillates. At the same time, the ratio of parameter inerements tends to a constant on approaching S from one side.

Table 4

n	s_n	δ_n^2
5	−2.44499	
6	−2.69146	
7	−2.65038	6.24564
8	−2.60895	7.26928
9	−2.69340	6.84839
10	−2.59842	7.04469
11	−2.70140	6.98638
12	−2.59671	7.02228
13	−2.70347	7.01160
14	−2.59517	7.02275
15	−2.70597	7.01216

Knowing these constants, we can find the break I corresponding to Eqs. (6.3) at the point G. Using the dependences s(I), constructed numerically in Section 4, we find that $I \approx 1.17$. Similar calculations for $z = 2$ showed that here, corresponding to the existence of quasi-periodic mode with rotation number σ we have the break $I \approx 1.47$. Phase portraits of this "torus" and of the "Cantorus" with the same rotation number, existing in the subcritical domain, are given above in Section 3, in Figs. 10 and 12 respectively.

Of course, the break I and Eqs. (6.3) is not a fixed quantity: it is equal to unity on the axis of symmetry $a = 0$, i.e., in the undisturbed system (6.1), and varies (apparently monotonely) on leaving this axis along the line S.

7. BIFURCATIONS IN RETURN MAPPINGS WITH A CHANGE OF ORIENTATION

In this section we shall briefly describe the bifurcation sequences in the case when the one-dimensional return mapping near one or both of the separatrices changes the orientation of intervals (i.e., for points x_1 and x_2 on the same side of the point $x = 0$, with $x_1 < x_2$ we have $F(x_1) > F(x_2)$).

Recall that a change of orientation is caused by a negative separatrix factor, i.e., by a negative coefficient of the principal term in the expansion of the branch of the return function near the saddle point. It is easily seen that a return mapping preserves the orientation after an even number of turns. We shall use the concept of loop orientability [36]. If, on formation of a j-turn loop of separatrix Γ_1 (Γ_2), the mapping $F^j(x)$ preserves the orientation for sufficiently small positive (negative) x, we call the loop orientable; if there is a change of orientation, the loop is non-orientable. If both separatrix factors are positive, all the loops are orientable, while if they are both negative, only loops with an even number of turns are orientable. If the separatrix factors have opposite sign, only those loops are orientable which include an even number of turns in the half-space with negative factor.

Accordingly, to the neighborhood of the point of intersection of lines of formation of orientable one-turn loops, there corresponds on the plane of parameters an orientable return mapping (Sections 2–5), while about the point of intersection of non-orientable loops we have the non-orientable case, and the situation close to the intersection of lines of orientable and non-orientable loops is called semi-orientable.

In the non-orientable case, when on both branches ($x < 0$ and $x > 0$) the return function F(x) is monotonely decreasing (Fig. 3c), the domain of the parameter plane in which the attractive modes are localized near the saddle, is bounded by three curves: the line of tangent bifurcation, generating a pair of two-turn cycles, and two lines on which the saddle separatrices hit an unstable two-turn cycle.

It is easily seen that, after two turns of the phase trajectory, the return function $F^2(x)$ is piecewise increasing, so that there is a large region in the domain described within which the dynamic behavior is exactly similar to the behavior analyzed above in the orientable case (Sections 2–6). The role of one-turn homoclinic loops of the orientable case is here played by the two-turn loops formed by separatrices which return to the saddle after making two turns in the same half-space (orientable loops 11 of separatrix Γ^+ and loops 00 of Γ^-).

The line of existence of each of these two-turn loops cuts transversally the line of formation of the one-turn non-oriented loop of the other separatrix, and around the point of intersection are observed structures typical of the semi-oriented case: an even number of turns (and preservation of the orientation in the relevant mapping) on one side of the saddle, and an odd number (with a change of orientation) on the other side.

Notice that, in the non-orientable (as distinct from the orientable) case, there are lines of period doubling of the cycles on the bifurcation diagram, though transition through a sequence of doublings is here again impossible: on any path to chaos we encounter not more than one doubling, because the eigenvalue of the linearization near the cycle with an even number of turns is necessarily non-negative.

We now indicate some specific features of the semi-orientable case. The separatrix factors here have opposite sign, so that the one-dimensional mapping is unimodal (Fig. 3d); on one side of point $x = 0$ the return function is increasing, on the other side it is decreasing, while at the point 0 itself it in general has a discontinuity: $F_+(0) \neq F_-(0)$.

From the point of intersection of one-turn loop lines a pencil of a countable set of curves departs on the parameter plane, with each curve corresponding to formation of a multi-turn non-orientable homoclinic loop. These lines cut one another and isolate on the plane a domain of dynamic behavior similar to that of the non-orientable case; the lines of

formation of orientable multi-turn loops, departing from the points of intersection, again cut one another, generating "islets" of orientable dynamics. Thus all the "quasi-periodic" and other modes, characterized above, can be encountered here. (It must however be noted that, in a small neighborhood of a point of intersection of one-turn loops, only cycles and homoclinic loops are encountered, and there are no "quasi-periodic" trajectories [27].)

Among the paths leading from regular behavior to chaos, there is a scenario which is only possible in the semi-orientable case. This is a sequence of period-doubling bifurcations; it corresponds to movement along the line $F_+(0) = F_-(0)$, on which the return mapping is continuous. From the mapping point of view this path is just the same as the usual Feigenbaum scenario (apart from the convergence law, see below), though in the initial continuous dynamic system we see the alternation of two types of bifurcation. Between every two period-doublings occurs the "passage" of a stable cycle through a stable manifold of the saddle point, i.e., the cycle merges into the right separatrix loop with simultaneous birth of a cycle with the same number of turns from the left separatrix loop (under the condition $F_+(0) = F_-(0)$ the loops of the two separatrices appear in pairs). In the mapping this bifurcation corresponds to the passage through "super-stability", i.e., passage of a point of the cycle from the domain $x > 0$ into the domain $x < 0$ via the point $x = 0$. It must be observed that, at the instant of bifurcation, the period of the cycle increases to infinity, though the length of the closed phase trajectory is naturally finite.

Let us dwell on the metric properties of this scenario. The similar Fiegenbaum renormalization transformation for the pair of functions

$$\begin{aligned} \eta(x) &= a_0 + a_1 x^z + a_2 x^{2z} + \ldots, \qquad x \geqslant 0 \\ \xi(x) &= b_0 + b_1 |x|^z + b_2 |x|^{2z} + \ldots, \quad x \leqslant 0 \end{aligned} \tag{7.1}$$

which satisfy the conditions $a_0 = b_0 > 0$, $a_1 < 0$, $b_1 < 0$, can be written as

$$R\begin{pmatrix}\eta(x)\\ \xi(x)\end{pmatrix} = \begin{pmatrix}\alpha\eta\xi\left(\dfrac{x}{\alpha}\right)\\ \alpha\eta\eta\left(\dfrac{x}{\alpha}\right)\end{pmatrix} \tag{7.2}$$

$$\alpha = \frac{\eta(0)}{\eta\xi(0)} < 0.$$

As distinct from the usual sequence of doublings, the extremum of the continuous mapping $F(x)$ is not in general quadratic. The asymptotic characteristics of the bifurcation sequence (convergence rate etc.) must therefore depend on the saddle index z, which defines this extremum. Even greater differences (reminiscent of the situation considered in Section 4) are caused by the fact that the functions $F_+(x)$ and $F_-(x)$ are not necessarily smoothly matched at the point $x = 0$. With $j > 1$, $a_j \neq b_j$, the mapping is continuous but not smooth. Here again arises a special kind of "break", equal to the ratio of separatrix factors

$$I_1(\eta, \xi) = \frac{\left.\dfrac{d\eta}{d(x^z)}\right|_{x=0}}{\left.\dfrac{d\xi}{d(|x|^z)}\right|_{x=0}} = \frac{a_1}{b_1}. \tag{7.3}$$

It is easily shown (see also [49]) that, under the action of transformation (7.2), the break I_1 becomes its inverse. Hence it is only in the symmetric case $I_1 = 1$ that the bifurcation sequence is convergent according to the law of a geometric progression, while in other situations the ratios of increments of the bifurcation values of the parameters must oscillate with period 2 (see [49] and Section 4 above). Obviously, the break I_1 is an invariant from the point of view of the double transformation

$$R^2\begin{pmatrix}\eta(x)\\ \xi(x)\end{pmatrix} = \begin{pmatrix}\beta^2\cdot\eta\xi\eta\eta\left(\dfrac{x}{\beta^2}\right)\\ \beta^2\cdot\eta\xi\eta\xi\left(\dfrac{x}{\beta^2}\right)\end{pmatrix} \tag{7.4}$$

$$\beta^2 = \frac{\eta(0)}{\eta\xi\eta\eta(0)} > 0.$$

It can be shown that the fixed point of this transformation satisfies the conditions $a_j = b_j\cdot(I_1)^j$, i.e., $\xi(x) = \eta(-x\cdot I_1^{-1/z})$. In the spectrum of eigenvalues of this point, one eigenvalue is unity (it corresponds to neutral perturbations, i.e., to a shift of the break), while two others are greater than unity. One of them determines the convergence rate of the sequence of bifurcation values of the parameter, $\mu_n \to \mu_{n+2} \to \mu_{n+4} \to \ldots$, while the other ($\gamma$) characterizes perturbations which violate the condition $a_0 = b_0$, i.e., destroy the continuity of the return

function at the point $x = 0$. Differentiation of Eqs. (7.4) with respect to x^z at the point $x = 0$ shows that $\gamma = \beta^{2z}$.

Thus the space of pairs of functions is fibered into subspaces, each of which is uniquely defined by the saddle index z and the break I_1. In each subspace the sequence of period-doubling bifurcations is characterized by a two-parameter scaling: the above-mentioned eigenvalues determine the ratio of "length" and "width" of the domain of stability of the 2^n-turn cycle with large n to the length and width of the domain of stability of the 2^{n+2}-turn cycle.

8. CONCLUSION

It has been shown that dissipative systems which have a saddle equilibrium state with separatrices returning to its neighborhood, can demonstrate very diverse dynamics when the parameters vary. Among the situations considered, those seem to be rather unusual when the systems are in a sense "conservative" and have a break I as the RG integral, while the attractive set is a trajectory similar to the winding of a two-dimensional torus with an irrational rotation number. We show the consequences resulting from a crossover, when the fixed point of the RG transformation is singular.

The fact that numerical integration of the continuous system fully confirms the quantitative as well as qualitative conclusions of our consideration reveals that the reduction to one-dimensional mappings is correct and means that we can expect the described sequences of transitions to be discoverable in other situations, say in distributed systems, and possibly in natural experiments.

Though our discussion has not been concerned with the chaotic motions that arise, it can be said with confidence that, close to the boundary of chaos, the properties of these motions will be described by scale-invariant laws, where the scaling constants are the above-defined eigenvalues of the linearized RG transformations, which characterize the scaling in the domain of regular behavior adjacent to the piece of boundary in question.

It can be said formally that a continuum of scenarios of transition to chaos is realized on the plane of parameters; in the orientable case, one such continuum corresponds to transitions with the formation of "quasi-periodic modes", and another, to transitions via a sequence of

imbedded domains. Nevertheless, there seem to be no special reasons for distinguishing qualitatively between scenarios within each of these groups — in the naive sense all the sequences of imbedding are similar to one another, and all the "quasi-periodic" modes are likewise similar. Only four types of boundary elements can be distinguished qualitatively from each other: apart from the two mentioned, there are the sides of the lobes that make up the boundary, i.e., the intervals in which transition to chaos occurs via intermittency, and intervals in which the regular motions undergo a boundary crisis. A similar crude division can be made in the continua of scenarios of the non-orientable and semi-orientable cases.

It has been assumed throughout our analysis that the variation of the parameters of the initial continuous system does not change the sign of the separatrix factor, i.e., the orientable case does not change into the semi-orientable case, etc. If the separatrix factors can change sign the bifurcation diagram is enriched and becomes more complicated; this would seem to be the explanation for the super-exponential sequence of bifurcations in the symmetric system of equations studied in [58].

Finally, the authors thank V.S. Afraimovich, M.I. Rabinovich, Ya.G. Sinai, and K.M. Khanin for interesting and stimulating discussions.

REFERENCES

1. Feigenbaum, M.J. (1978) Quantitative Universality for a Class of Nonlinear Transformations, *J. Stat. Phys.*, **19**, 25–51.
2. Feigenbaum, M.J. (1983) Universal Behavior in Nonlinear Systems, *Physica*, **7D**, 16–39.
3. Pomeau, Y. and Manneville, P. (1980) Intermittent Transition to Turbulence in Dissipative Dynamical Systems, *Commun. Math. Phys.*, **74**, 189–197.
4. Eckmann, J.-P. (1981) Roads to Turbulence in Dissipative Dynamical Systems, *Rev. Mod. Phys.*, **53**, 643–654.
5. Afraimovich, V.S. and Shil'nikov, L.P. (1974) On some global bifurcations connected with the disappearance of a fixed point of the saddle-node type, *Dokl. Akad. Nauk SSSR*, **219**, 1281–1286.
6. Afraimovich, V.S. and Shil'nikov, L.P. (1983) Invariant two-dimensional tori, their destruction and stochasticity, in the book: Methods of qualitative theory of differential equations, *Gor'kii*, 3–26.
7. Ostlund, S. *et al.*, (1983) Universal Properties of the Transition from Quasi-periodicity to Chaos in Dissipative Systems, *Physica*, **8D**, 303–342.
8. Feigenbaum, M.J. *et al.* (1982) Quasiperiodicity in Dissipative Systems: a Renormalization Group Analysis, *Physica*, **5D**, 370–386.

9. Golberg, A.I. *et al.* (1983) Universal Properties of the Sequences of Period-Tripling Bifurcations, *Russian Math. Surv.*, **38**.
10. Chang, Sh.-J. *et al.* (1982) Tricritical Points and Bifurcations in a Quartic Map. In: Nonlinear Problems: Present and Future, *North Holland Publ. Co.*, 395–402.
11. Lichtenberg, A.J. and Lieberman, M.A. (1982) Regular and Stochastic Motion, *Appl. Math. Sci.*, **38**, Springer-Verlag.
12. Vul, E.B. *et al.* (1984) The Feigenbaum Universality and Thermodynamical Formalism, *Russian Math. Surv.*, 39, 1–40.
13. Hu, B. (1982) Introduction to Real-space Renormalization-Group Methods in Critical and Chaotic Phenomena, *Phys. Repts.*, **91**, 233–295.
14. Lorenz, E.N. (1963) Deterministic Nonperiodic Flow, *J. Atmos. Sci.*, **20**, 130–141.
15. Shilnikov, L.P. (1965) A Case of the Existence of a Denumerable Set of Periodic Motions, *Soviet Math. Dokl.*, 6, 163–166.
16. Shilnikov, L.P. (1970) A Contribution to the Problem of the Structure of an Extended Neighborhood of a Rough Equilibrium State of Saddle-Focus Type, *Math. USSR. Sbornik*, **10**, 91–102.
17. Shilnikov, L.P. (1968) On the Generation of a Periodic Motion from Trajectories Doubly Asymptotic to an Equilibrium State of Saddle Type, *Math. USSR. Sbornik*, **6**, 428–438.
18. Gaspard, P. (1983) Generation of a Countable Set of Homoclinic Flows through Bifurcation, *Phys. Lett.*, **97A**, 1–4.
19. Glendinning, P. and Sparrow, C. (1984) Local and Global Behavior near Homoclinic Orbits, *Journ. Stat. Phys.*, **35**, 645–695.
20. Gaspard, P. *et al.* (1984) Bifurcation Phenomena near Homoclinic Systems: A Two-Parameter Analysis, *Journ. Stat. Phys.*, **35**, 697–727.
21. Ovsyannikov, I.M. and Shil'nikov, L.P. (1986) On systems with a homoclinic curve of saddle-focus type. *Mathematicheskii Sbornik*, **130**, 552–570.
22. Williams, R.F. (1977) The Structure of Lorenz Attractors, *Lecture notes in Math.*, **615**, 93–113.
23. Afraimovich, V.S. *et al.* (1977) On the Origin and Structure of the Lorenz Attractor, *Sov. Phys. Dokl.*, **22**, 253–256.
24. Yorke, E. and Yorke, J. (1979) Metastable Chaos: Transition to Sustained Chaotic Behavior in the Lorenz Model, *J. Stat. Phys.*, **21**, 263–277.
25. Afraimovich, V.S. *et al.* (1980) On attracting limit sets of the Lorenz attractor type. *Trudy Moskovskogo matemat obshchestva*, **44**, 150–212.
26. Sparrow, C. (1982) The Lorenz Equations: Bifurcations, Chaos and Strange Attractors, *Appl. Math. Sci.*, **41**, Springer, Berlin.
27. Turaev, D.V. and Shil'nikov, L.P. (1986) On the bifurcations of a homoclinic "figure of eight" of a saddle with negative saddle value, *Dokl. Akad. nauk SSSR*, **290**, 1301–1304.
28. Arneodo, A. *et al.* (1981) A Possible New Mechanism for the Onset of Turbulence, *Phys. Lett.*, **81A**, 197–201.
29. Lyubimov, D.V. and Zaks, M.A. (1983) Two Mechanisms of the Transition to Chaos in Finite-Dimensional Models of Convection, *Physica*, **9D**, 52–64.
30. Tresser, C. (1983) Nouveaux types de Transitions vers une Entropie Topologique positive, *C. R. Acad. Sci. Paris*, t 296, Ser. 1, 729–732.
31. Procaccia, I. *et al.* (1987) First-Return Maps and a Unified Renormalization Scheme for Dynamical Systems, *Phys. Rev. A*, **35**, 1884–1900.
32. Grebogi, C. *et al.* (1983) Sudden Changes in Chaotic Attractors and Transient Chaos, *Physica*, **7D**, 181–200.
33. Arnol'd, V.I. *et al.* (1985) Mathematical Aspects of Classical and Celestial Mechanics, Moscow, Izd-vo VINITI.

34. Kuramoto, Y., and Koga, S. (1982) Anomalous Period-Doubling Bifurcations Leading to Chemical Turbulence, *Phys. Lett.*, **92A**, 1–4.
35. Turaev, D.V. (1984) On a case of bifurcations of a contour formed by homoclinic curves of a saddle, in the book: Methods of the Qualitative Theory of Differential Equations, Gor'kii, 162–175.
36. Shilnikov, L.P. (1980) Theory of Bifurcations and the Lorenz Model. Appendix to the Russian edition of: J.E. Marsden, M. McCracken "The Hopf Bifurcation and Its Applictions", Moscow, *Mir*, 317–335.
37. Collet, P. and Eckmann, J.-P. (1980) *Iterated Maps on the Interval as Dynamical Systems*, Boston, Birkhauser.
38. Singer, D. (1978) Stable Orbits and Bifurcations of Maps of the Interval, *SIAM J. Appl. Math.*, **35**, 260–267.
39. Collet, P. *et al.* (1985) Scenarios under Constraint *J. de Phys.-Lettr.*, t 46, L143–148.
40. Nitecky, Z. (1971) Differentiable Dynamics: an Introduction. Cambridge, the MIT Press.
41. Arnold, V.I. (1978) Supplementary Chapters to the Theory of Ordinary Differential Equations. Moscow, Nauka publishers.
42. Keener, J.P. (1980) Chaotic Behavior in Piecewise Continuous Difference Equations, *Trans. Amer. Math. Soc.*, **261**, 589–604.
43. Gambaudo, J.-M. and Tresser, C. (1985) Dynamique Reguliere ou Chaotique, *C. R. Acad. Sci. Paris*, Th. 300, Ser. 1, 311–314.
44. Malkin, M.I. (1986) Intervals of rotation and the dynamics of mappings of Lorenz type, in the book: Methods of the Qualitative Theory of Differential Equations, Gor'kii, 122–139.
45. Jensen, M. *et al.* (1983) Complete Devil's Staircase, Fractal Dimension and Universality of Mode-Locking Structure in the Circle Map, *Phys. Rev. Lett.*, **50**, 1637–1639.
46. Cornfeld, I.P. *et al.* (1982) *Ergodic Theory*. Berlin, Springer.
47. Derrida, B. *et al.* (1979) Universal Metric Properties of Bifurcations of Endomorphisms, *J. Phys. A*, **12**, 269–296.
48. Gambaudo, J.-M. *et al.* (1986) New universal Scenarios for the Onset of Chaos in Lorenz-Type Flows, *Phys. Rev. Lett.*, **57**, 925–928.
49. Arneodo, A. *et al.* (1979) A Renormalization Group with Periodic Behavior, *Phys. Lett.*, **70A**, 74–76.
50. Farmer, J.D. and Satija, I. (1985) Renormalization of the Quasiperiodic Transition to Chaos for Arbitrary Winding Numbers, *Phys. Rev. A*, **31**, 3520–3522.
51. Cvitanovic, P. *et al.* (1985) Renormalization, Unstable Manifolds and the fractal Properties of Mode Locking, *Phys. Rev. Lett.*, **55**, 343–346.
52. Monin, A.S. and Yakobson, M.V. (1986) On local fractality, *Dokl. Akad. nauk SSSR*, **287**, 795–798.
53. Zisook, A. (1981) Universal Effects of Dissipation in Two-Dimensional Mappings, *Phys. Rev. A*, **24**, 1640–1642.
54. Cherry, T. (1938) Analytic Quasiperiodic Curves of Discontinuous Type on a Torus, *Proc. London Math. Soc.*, **44**, 175–215.
55. Aranson, S.Kh. (1986) On topological structure of Cherry flows on a torus, *Funkts. Anal. i Prilozh.*, **20**, 62–63.
56. Zaks, M.A. *et al.* (1983) On the influence of vibrations on over-critical convection modes, *Izv. Akad. Nauk SSSR, Fizika atmosfery i okeana*, **19**, 312–314.
57. Gershuni, G.Z. and Zhukhovitsky, E.M. (1972) Convective Stability of Incompressible Fluids, Moscow, Nauka publ.
58. Coste, J. and Peyraud, N. (1982) A New Type of Period-Doubling Bifurcations in One-Dimensional Transformations with Two Extrema, *Physica*, **5D**, 415–420.

INDEX

Soviet Scientific Reviews, Section C
Mathematical Physics Reviews

Contents, Volume 1

Contents, Volume 2